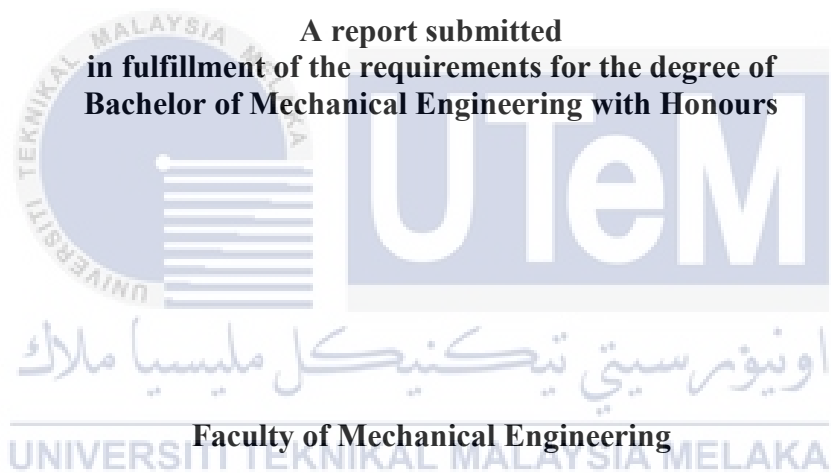


**STUDY OF COMPUTATIONAL FLUID DYNAMICS ON PHOTOVOLTAIC
THERMAL SOLAR WATER COLLECTOR**

YAP JOON PING

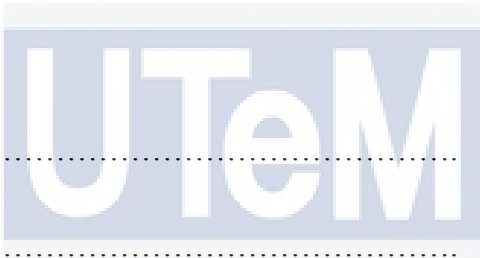


UNIVERSITI TEKNIKAL MALAYSIA MELAKA

2018

DECLARATION

I declare that this project report entitled “Study of Computational Fluid Dynamics on Photovoltaic Thermal Solar Water Collector” is the result of my own work except as cited in the references.



Signature :

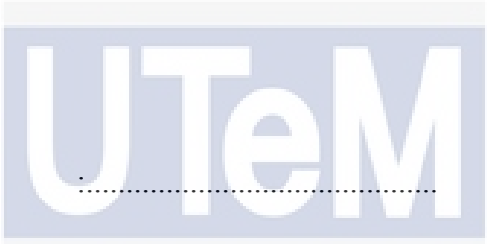
Name :

Date : اونيومر ستي تيكنيكل مليسيا ملاك

UNIVERSITI TEKNIKAL MALAYSIA MELAKA

SUPERVISOR'S DECLARATION

I hereby declare that I have read this project report and in my opinion this report is sufficient in terms of scope and quality for the award of the degree of Bachelor of Mechanical Engineering with Honours.



Signature :

Supervisor's Name :

Date :

اونيورسيتي تیکنیکل ملیسیا ملاک

UNIVERSITI TEKNIKAL MALAYSIA MELAKA

DEDICATION

To my beloved mother and father



ABSTRACT

The purpose of this research is to investigate the performance of photovoltaic thermal collector with different design of absorber tube in steady state condition. ANSYS Fluent software was used to carry out computational fluid dynamics (CFD) simulation. In this study, water was selected as the heat transfer fluid. The geometric model was drawn in CATIA V5R20 and imported into ANSYS software to generate mesh model. In setup of simulation, the viscous model, radiation model and material properties were constructed. Flow of heat transfer fluid was laminar flow. In radiation model, surface to surface (S2S) model was used. The photovoltaic panel used in this research was silicon based photovoltaic cell. Validation was carried out by referring to the previous work. In the comparison between author simulation results and previous simulation results, the root mean square error was 2.52 °C. On the other hand, the root mean square error was 1.29°C in comparison between current simulation results and previous experimental results. The root mean square error between previous research simulation and previous experimental results is 2.08°C. The influences of mass flow rate and solar irradiance intensity on performance PVT was determined. Spiral absorber PVT has the highest total efficiency at most of the mass flow rate among the three design of absorber and followed by vertical serpentine absorber and then horizontal serpentine absorber.

اونيورسيتي تيكنيكل مليسيا ملاك

UNIVERSITI TEKNIKAL MALAYSIA MELAKA

ABSTRAK

Tujuan penyelidikan ini adalah untuk mengkaji prestasi pengumpul haba photovoltaic dengan reka bentuk tiub penyerap yang berbeza dalam keadaan mantap. Perisian ANSYS Fluent telah digunakan untuk menjalankan simulasi cecair dinamik (CFD). Dalam kajian ini, air dipilih sebagai cecair pemindahan haba. Model geometri telah dilukis dalam CATIA V5R20 dan diimport ke perisian ANSYS untuk menghasilkan model mesh. Dalam “setup”, model aliran, model radiasi dan sifat bahan telah dibina. Aliran cecair pemindahan haba adalah aliran laminar. Dalam model radiasi, model permukaan ke permukaan (S2S) telah digunakan. Panel photovoltaic yang digunakan dalam penyelidikan ini adalah sel photovoltaic silikon. Pengesahan telah dilakukan dengan merujuk kepada penyelidikan sebelumnya. Dalam perbandingan antara keputusan simulasi semasa dan keputusan simulasi sebelumnya, perbezaan peratusan tertinggi ialah 9.33%. Sebaliknya, ralat peratusan tertinggi ialah 6.89% berbanding keputusan simulasi semasa dan keputusan eksperimen terdahulu. Pengaruh kadar aliran jisim dan keamatan sinar matahari terhadap prestasi PVT ditentukan. PVT penyerap lingkaran mempunyai kecekapan keseluruhan yang tertinggi dalam kebanyakan kadar aliran jisim di antara tiga reka bentuk penyerap, dan diikuti oleh penyerap serpent menegak dan penyerap serpent mendatar.

ACKNOWLEDGEMENTS

I would like to express my sincere appreciation to my supervisor Dr. Mohd Afzanizam Bin Mohd Rosli from Faculty of Mechanical Engineering Universiti Teknikal Malaysia Melaka for his guidance, advice, as well as support provided to me throughout this research.

Beside my supervisor, I would also love to express my gratitude to Dr Tee Boon Tuan and Dr Fudhail Bin Abdul Munir that have provided me with solutions and advices at difficult times faced throughout this research.

I would also like to thank my fellows who willing spend their precious time to teach me step by step of the procedure of simulation software patiently and share the knowledge with me.

Last but not least, I would like to thank my family members that have been always supporting me spiritually throughout my life.



TABLE OF CONTENTS

	PAGE
DECLARATION	
SUPERVISOR'S DECLARATION	
DEDICATION	
ABSTRACT	i
ABSTRAK	ii
ACKNOWLEDGEMENTS	iii
TABLE OF CONTENTS	iv
LIST OF TABLES	vi
LIST OF FIGURES	viii
LIST OF APPENDICES	x
LIST OF ABBREVIATIONS	xi
LIST OF SYMBOLS	xii
LIST OF PUBLICATIONS	xiii
CHAPTER 1	1
INTRODUCTION	1
1.1 Background	1
1.2 Problem Statement	2
1.3 Objectives	3
1.4 Scopes	3
CHAPTER 2	4
LITERATURE REVIEW	4
2.1 Photovoltaic Cell	4
2.2 Solar Thermal Collector	6
2.2.1 Energy Analysis of Solar Thermal Collector	7
2.3 Photovoltaic Thermal Hybrid Solar Collector	9
2.3.1 Photovoltaic Thermal Solar Water Collector	10
2.3.2 Photovoltaic Thermal Solar Air Collector	11
2.4 Improvement on PVT	11
2.4.1 Application of New Design of Absorber	11
2.4.2 Application of Concentrator	12

2.5	Comparison of Study	13
CHAPTER 3		14
METHODOLOGY		14
3.1	Introduction	14
3.2	Geometry Drawing	16
3.3	Meshing	18
3.4	Pre-processing	19
3.5	Post-processing	20
3.6	Mathematics Calculation	21
3.7	Validation	22
CHAPTER 4		24
RESULTS AND DISCUSSION		24
4.1	Influence of Mass Flow Rate on Thermal Efficiency	24
4.2	Influence of Mass Flow Rate on Photovoltaic Panel Efficiency	34
4.3	Influence of Radiation on PVT	43
4.4	Performance of PVT	46
CHAPTER 5		48
CONCLUSION AND RECOMMENDATIONS		48
5.1	Conclusion	48
5.2	Recommendations	49
REFERENCES		50
APPENDICES		53

LIST OF TABLES

TABLE	TITLE	PAGE
Table 2.1	Efficiency of Different Type of Photovoltaic Cell (Stylianou, 2016)	5
Table 2.2	Comparison of Study	13
Table 3.1	Dimension of PVT Components	18
Table 3.2	Material Properties of PVT Components (Nahar et al., 2017)	20
Table 3.3	Comparison of Results for Validation	23
Table 4.1	Results of Outlet Temperature and Thermal Efficiency of Horizontal Serpentine Absorber under $1000\text{W}/\text{m}^2$ Solar Irradiance	26
Table 4.2	Results of Outlet Temperature and Thermal Efficiency of Vertical Serpentine Absorber under $1000\text{W}/\text{m}^2$ Solar Irradiance	27
Table 4.3	Results of Outlet Temperature and Thermal Efficiency of Spiral Absorber under $1000\text{W}/\text{m}^2$ Solar Irradiance	27
Table 4.4	Results of Outlet Temperature and Thermal Efficiency of Horizontal Serpentine Absorber under $800\text{W}/\text{m}^2$ Solar Irradiance	29
Table 4.5	Results of Outlet Temperature and Thermal Efficiency of Vertical Serpentine Absorber under $800\text{W}/\text{m}^2$ Solar Irradiance	30
Table 4.6	Results of Outlet Temperature and Thermal Efficiency of Spiral Absorber under $800\text{W}/\text{m}^2$ Solar Irradiance	30
Table 4.7	Results of Outlet Temperature and Thermal Efficiency of Horizontal Serpentine Absorber under $600\text{W}/\text{m}^2$ Solar Irradiance	32
Table 4.8	Results of Outlet Temperature and Thermal Efficiency of Vertical Serpentine Absorber under $600\text{W}/\text{m}^2$ Solar Irradiance	32
Table 4.9	Results of Outlet Temperature and Thermal Efficiency of Spiral Absorber under $600\text{W}/\text{m}^2$ Solar Irradiance	33
Table 4.10	Results of PV Temperature and PV Efficiency of Horizontal Serpentine Absorber under $1000\text{W}/\text{m}^2$ Solar Irradiance	36
Table 4.11	Results of PV Temperature and PV Efficiency of Vertical Serpentine Absorber under $1000\text{W}/\text{m}^2$ Solar Irradiance	37
Table 4.12	Results of PV Temperature and PV Efficiency of Spiral Absorber under $1000\text{W}/\text{m}^2$ Solar Irradiance	37

Table 4.13 Results of PV Temperature and PV Efficiency of Horizontal Serpentine Absorber under $800\text{W}/\text{m}^2$ Solar Irradiance	39
Table 4.14 Results of PV Temperature and PV Efficiency of Vertical Serpentine Absorber under $800\text{W}/\text{m}^2$ Solar Irradiance	39
Table 4.15 Results of PV Temperature and PV Efficiency of Spiral Absorber under $800\text{W}/\text{m}^2$ Solar Irradiance	40
Table 4.16 Results of PV Temperature and PV Efficiency of Horizontal Serpentine Absorber under $600\text{W}/\text{m}^2$ Solar Irradiance	41
Table 4.17 Results of PV Temperature and PV Efficiency of Vertical Serpentine Absorber under $600\text{W}/\text{m}^2$ Solar Irradiance	41
Table 4.18 Results of PV Temperature and PV Efficiency of Spiral Absorber under $600\text{W}/\text{m}^2$ Solar Irradiance	42



LIST OF FIGURES

FIGURE	TITLE	PAGE
Figure 2.1	Types of Silicon Photovoltaic Panels	4
Figure 2.2	Cross-section of Glazed PVT (Kim & Kim, 2012)	7
Figure 2.3	Cross-section of Unglazed PVT (Kim & Kim, 2012)	7
Figure 2.4	Heat Flow through Solar Thermal Collector	7
Figure 2.5	Main Components of PVT Collector	10
Figure 3.1	Flow chart of the Methodology	15
Figure 3.2	Horizontal Serpentine Absorber in CATIA Part Design	16
Figure 3.3	Vertical Serpentine Absorber in CATIA Part Design	16
Figure 3.4	Spiral Absorber in CATIA Part Design	17
Figure 3.5	Cross-section of Absorber	17
Figure 3.6	Exploded View of PVT	17
Figure 4.1	Contour Diagram of PV of spiral absorber PVT at 0.0005 kg/s under $1000W/m^2$ solar irradiance	24
Figure 4.2	Contour Diagram of water surface of spiral absorber PVT at 0.0005 kg/s under $1000W/m^2$ solar irradiance	24
Figure 4.3	Contour Diagram of PV of spiral absorber PVT at 0.005 kg/s under $1000W/m^2$ solar irradiance	25
Figure 4.4	Contour Diagram of water surface of spiral absorber PVT at 0.005 kg/s under $1000W/m^2$ solar irradiance	25
Figure 4.5	Changes in Temperature Difference and Thermal Efficiency with Various Mass Flow Rate under $1000W/m^2$ Solar Irradiance	28
Figure 4.6	Changes in Temperature Difference and Thermal Efficiency with Various Mass Flow Rate under $800W/m^2$ Solar Irradiance	31
Figure 4.7	Changes in Temperature Difference and Thermal Efficiency with Various Mass Flow Rate under $600W/m^2$ Solar Irradiance	33
Figure 4.8	Contour Diagram of PV of spiral absorber PVT at 0.005 kg/s under $1000W/m^2$ solar irradiance	34

Figure 4.9 Contour Diagram of water surface of spiral absorber PVT at 0.005 kg/s under $1000W/m^2$ solar irradiance	34
Figure 4.10 Contour Diagram of PV of spiral absorber PVT at 0.005 kg/s under $600W/m^2$ solar irradiance	35
Figure 4.11 Contour Diagram of PV of spiral absorber PVT at 0.005 kg/s under $600W/m^2$ solar irradiance	35
Figure 4.12 Changes in PV Temperature and PV Efficiency with Various Mass Flow Rate under $1000W/m^2$ Solar Irradiance	38
Figure 4.13 Changes in PV Temperature and PV Efficiency with Various Mass Flow Rate under $800W/m^2$ Solar Irradiance	40
Figure 4.14 Changes in PV Temperature and PV Efficiency with Various Mass Flow Rate under $600W/m^2$ Solar Irradiance	42
Figure 4.15 Evolution of Thermal Efficiency with Intensity of Solar Irradiance at Mass Flow Rate of 0.005 kg/s	43
Figure 4.16 Evolution of PV Efficiency with Intensity of Solar Irradiance at Mass Flow Rate of 0.005 kg/s	44
Figure 4.17 Evolution of Total Efficiency with Intensity of Solar Irradiance at Mass Flow Rate of 0.005 kg/s	45
Figure 4.18 Evolution of Total Efficiency under $1000W/m^2$ Solar Irradiance Intensity	46
Figure 4.19 Evolution of Total Efficiency under $800W/m^2$ Solar Irradiance Intensity	46
Figure 4.20 Evolution of Total Efficiency under $600W/m^2$ Solar Irradiance Intensity	47

LIST OF APPENDICES

APPENDIX	TITLE	PAGE
A	PSM I Gantt Chart	55
B	PSM II Gantt Chart	56
C	Contour Diagram of PV surface and water surface of spiral absorber PVT at 0.005 kg/s under $1000W/m^2$ solar irradiance	57
D	Contour Diagram of PV surface and water surface of vertical serpentine absorber PVT at 0.005 kg/s under $1000W/m^2$ solar irradiance	58
E	Contour Diagram of PV surface and water surface of horizontal serpentine absorber PVT at 0.005 kg/s under $1000W/m^2$ solar irradiance	59
F	Contour Diagram of PV surface and water surface of spiral absorber PVT at 0.0005 kg/s under $1000W/m^2$ solar irradiance	60
G	Contour Diagram of PV surface and water surface of vertical serpentine absorber PVT at 0.0005 kg/s under $1000W/m^2$ solar irradiance	61
H	Contour Diagram of PV surface and water surface of horizontal serpentine absorber PVT at 0.0005 kg/s under $1000W/m^2$ solar irradiance	62

LIST OF ABBEREVATIONS

CAD	Computer-Aided Design
CdTe	Cadmium Telluride
CFD	Computational Fluid Dynamic
CIGS	Copper Indium Gallium Selenide
CPVT	Concentrated Photovoltaic Thermal
c-Si	Monocrystalline Silicon
HTF	Heat Transfer Fluid
pc-Si	Polycrystalline Silicon
PV	Photovoltaic
PVT	Photovoltaic Thermal
PVT/a	Photovoltaic Thermal Air
PVT/w	Photovoltaic Thermal water



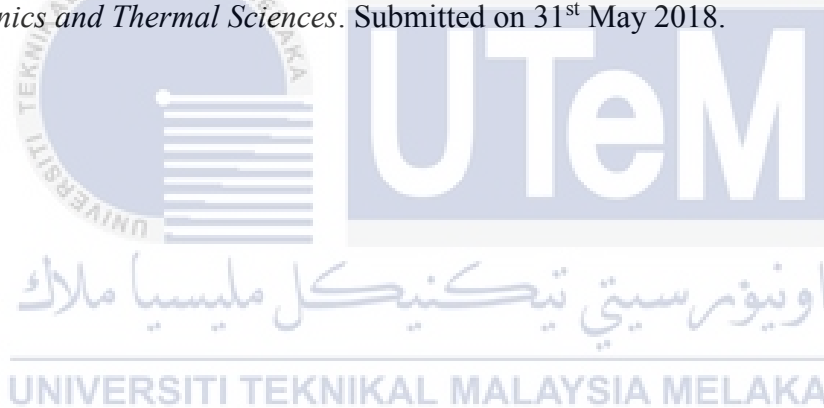
LIST OF SYMBOLS

α	-	Absorptance
β_{ref}	-	Temperature coefficient
η_{Total}	-	Total efficiency
η_{pv}	-	Electrical efficiency / photovoltaic cell efficiency
η_{ref}	-	Reference efficiency
η_{th}	-	Thermal efficiency
τ	-	Transmittance
A	-	Area
F_R	-	Heat removal factor
h	-	Heat transfer coefficient
I	-	Intensity of irradiance
\dot{m}	-	Mass flow rate
Q_i	-	Heat gain
Q_o	-	Heat loss
Q_u	-	Useful energy
q	-	Heat flux
T_a	-	Ambient temperature
T_c	-	Photovoltaic Cell temperature
T_{col}	-	Collector temperature
T_i	-	Inlet temperature
T_o	-	Outlet temperature
T_{ref}	-	Reference temperature
U_L	-	Overall heat transfer coefficient
v	-	Velocity
V	-	Volume

LIST OF PUBLICATIONS

Joon Ping, Y., Afzanizam, M., Rosli, M., & Saruni, M. A. (2018). Preliminary study of computational fluid dynamics on photovoltaic thermal solar air collector. *Proceedings of Mechanical Engineering Research Day*, (May), 175–177.

Joon Ping, Y., Afzanizam, M., Rosli, M., & Saruni, M. A. (n.d.). Simulation Study of Computational Fluid Dynamics on Photovoltaic Thermal Water Collector with Different Designs of Absorber Tube. *Journal of Advanced Research in Fluid Mechanics and Thermal Sciences*. Submitted on 31st May 2018.



CHAPTER 1

INTRODUCTION

1.1 Background

The research on renewable energy has been going on for decades and solar energy is one of the most researched field since it is clean and easily obtainable and almost inexhaustible for another 5 billion years. Solar energy should be used to substitute the energy obtained from burning fossil fuels to reduce the environmental pollution and global warming.

Currently, the harvesting of solar energy is divided into two main categories, which is by using the photovoltaics (PV) system or the solar thermal system. The difference between those two is that PV system uses solar energy to generate electrical energy while solar thermal system is for generating thermal energy. With the combination of both systems, photovoltaic thermal (PVT) system is introduced. This system able to generate electric energy while converting the heat lost to the surrounding into thermal energy, this may cool down the PV system to provide a better efficiency. The PVT system can also improve the appearance of roofs and requires a lower cost compared to installing PV system and solar thermal collector separately (Khelifa et al., 2016). The PVT system can be further classified into two category which is glazed PVT collector and unglazed PVT collector. Generally, the glazed PVT collector will produce more heat energy but is lower in electrical efficiency. On the other hand, unglazed PVT collector will yield less thermal energy but generate more electric energy (Kim & Kim, 2012).

The study of fluid dynamics is also critical during this research as it allows better understanding and design of the system. With the help of Computational Fluid Dynamics (CFD), numerical analysis and data structure was used to simulate the design and perform lengthy calculations. Since all experiments were done inside a virtual flow laboratory, by simply changing the variables, the characteristic changes of the fluid can be visualized. Therefore, optimization can be made to improve the designed model. Simulation using CFD can obtain results without carry out costly and time-consuming real experiment.

1.2 Problem Statement

Global warming is one of the most serious issues that the world facing today. The main cause of global warming is the emission of greenhouse gases from burning fossil fuel to provide electric energy. Moreover, these non-renewable resources are finite, and it will eventually run out. Renewable energy, for instance, solar energy, wind energy and hydropower are better choices to replace the non-renewable energy.

Photovoltaic thermal hybrid solar collector is a system which can convert solar radiation into heat and electric energy simultaneously by using solar collector and photovoltaic panel. However, at high temperature, the performance of photovoltaic panels will be reduced but while at low temperature, the solar collector will underperform. The purpose of this project is to achieve optimum performance on photovoltaic panel and thermal collector. With the aid of CFD, the results can be predicted without using the actual PVT. If the results are not desired, no resources will be wasted, and improvement can be made based on the results. According to Kim & Kim (2012), the average thermal and electrical efficiency of glazed PVT collector is 48.4% and unglazed PVT collector has 35.8%. The efficiency of both unglazed PVT and glazed PVT are less than 50%. This means that there are more than 50% of energy is lost.

1.3 Objectives

The objectives of this project are:

1. To design new absorber tube of flat plate photovoltaic thermal hybrid solar collector.
2. To determine the overall performance of PVT.
3. To determine the relationship of heat transfer fluid mass flow rate and solar irradiance intensity against performance of PVT.

1.4 Scopes

The scopes of this project are:

1. Simulation will be conducted on glazed photovoltaic thermal collector.
2. The serpentine and spiral design of absorber tube will be used in photovoltaic thermal collector.
3. Absorber tube with one inlet and one outlet will be used in simulation.
4. Length of absorber tube will be fixed at 4.8m.
5. Simulation will be performed under steady state.
6. Bottom of absorber tube is assumed as adiabatic, hence insulation is not included in simulation.

CHAPTER 2

LITERATURE REVIEW

2.1 Photovoltaic Cell

Photovoltaic cell, also known as solar cell convert the light received to electrical energy, this process is known as photovoltaic effect. The photovoltaic cell is treated semiconductor in positive side (P-type) and negative side (N-type). When photon or light strike on photovoltaic cell, electron from N-type will be dislodged. As the dislodged electron move to P-type, flow of electric current is formed.



Figure 2.1 Types of Silicon Photovoltaic Panels

Mostly of the photovoltaic cells are made up of crystalline silicon which are monocrystalline silicon (c-Si) and polycrystalline silicon (pc-Si). Figure 2.1 shows c-Si, pc-Si and amorphous photovoltaic panels. Monocrystalline photovoltaic cells are the most efficient among all type of the commercial photovoltaic cells. Monocrystalline is in shape of hexagon which is black in colour, therefore it can fit well in photovoltaic panel and increase the light absorption. Because of its high efficiency, the space required to yield a certain

amount of power output is relatively lesser. It also has the greater durability and perform better in low light but it is more expensive than other photovoltaic cells. Efficiency range of monocrystalline photovoltaic cell is between 15% and 29%. Polycrystalline photovoltaic cell is blue colour because of the anti-reflective layer which used to ensure the maximum adsorption of light. It has the efficiency of 13-15%. Amorphous silicon photovoltaic cell is a non-crystalline silicon and is a type of the thin film PV. Its efficiency is far lesser than crystalline silicon photovoltaic cell, only from 5 to 8%. Besides amorphous photovoltaic cell, the other types of thin film photovoltaic cell are cadmium telluride (CdTe) and copper indium gallium selenide (CIGS). As ease of manufacturing and abundant of cadmium telluride photovoltaic cell, now it is the second most utilized material in manufacturing of photovoltaic panel, followed by silicon. However, their efficiency is relatively lower than crystalline silicon photovoltaic cell. Table 2.1 indicates the efficiency of different types of photovoltaic cell in normal and laboratory condition.

Table 2.1 Efficiency of Different Type of Photovoltaic Cell (Stylianou, 2016)

Technology	Mono c-Si	Poly c-Si	GaAs	a-Si thin film	CIS/CIGS thin film	CdTe thin film	Organic	Dye-sensitized	Multi-junction
Generation	1 st	1 st	1 st	2 nd	2 nd	2 nd	3 rd	3 rd	3 rd
Commercial cell efficiency (%)	15-29	13-15	N/A	5-8	7-11	8-11	3-4	1-5	25-30
Best laboratory cell efficiency (%)	25	20.4	26.4	13.4	20.4	19.6	11.1	11.4	37.9

The electrical efficiency of photovoltaic cells is strongly affected by operating temperature and irradiance or light intensity. According to Skoplaki & Palyvos (2009) and Daghigh, Ibrahim, Jin, Ruslan, & Sopian (2011), the electrical efficiency decreases linearly with operating temperature and irradiance. Experimental study has been conducted to determine the effect of light intensity on performance of photovoltaic cell (Khan, Singh, &

Husain, 2010). The study shows that the performance of photovoltaic cell is decreases with illumination intensity. However, the rate of decrease is lower at higher illumination intensity.

2.2 Solar Thermal Collector

The solar thermal collector is a device that utilizes solar radiation to heat air or water for space heating and domestic water heating purposes. There are many different types of solar thermal collector. The flat-plate collector is the most common solar thermal collector.

The main components of flat plate collector comprised of glazing cover, absorber plate, tubes, and insulation. The glazing cover is transparent and is normally made up of glass or plastic. The glazing cover helps to minimize the convection and radiation heat loss and protect the thermal collector from harsh weather. The surface of absorber plate is treated with black colour coating for maximizing the heat absorption. Absorber tubes act as channel for heat transfer fluid (HTF) to pass through the solar thermal collector. Absorber tube and absorber plate are welded together to allow heat transfer between fluid and absorber. While the bottom and sides of flat plate collector is cover by insulated casing to prevent heat loss. Absorber tubes in harp and serpentine design is the common design in the commercial solar collectors.

A flat plate collector without glazing cover is known as unglazed solar thermal collector whereas flat plate collector with glazing cover is known as a glazed solar collector. Cross-section of glazed and unglazed PVT collector is shown in Figure 2.2 and Figure 2.3 respectively. Unglazed solar collector costs less compared to glazed solar collector but it has poor performance in cold or windy weather. According to Kim & Kim (2012), several experiments were carried out to compare the performance of unglazed PVT collector and glazed PVT collector and conclude that the unglazed PVT collector has the better electrical

efficiency whereas glazed PVT collector has the better thermal efficiency. However, the total efficiency of glazed PVT collectors is still higher, it has efficiency of 48.4%, while unglazed PVT collector has only 35.8%.

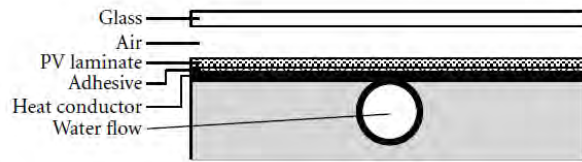


Figure 2.2 Cross-section of Glazed PVT (Kim & Kim, 2012)

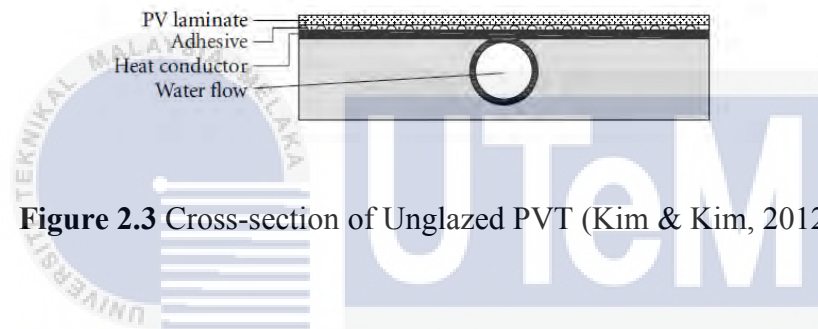


Figure 2.3 Cross-section of Unglazed PVT (Kim & Kim, 2012)

2.2.1 Energy Analysis of Solar Thermal Collector

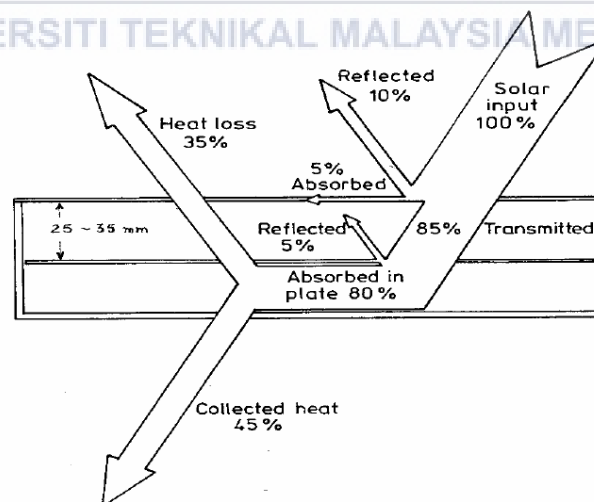


Figure 2.4 Heat Flow through Solar Thermal Collector

Figure 2.4 illustrate schematic diagram of heat flow through flat plate solar collector.

$$Q_i = I \cdot A$$

Q_i is the heat gained by collector when intensity of solar radiation, I strikes the surface of collector with a surface area, A . However, every surface of material has its transmittance and absorption, thus only partial radiation will transmit through the material and some will be absorbed by the material. Hence,

$$Q_i = I(\tau\alpha) \cdot A$$

When collector absorb heat until its temperature is higher than the ambient temperature, heat loss occurred.

$$Q_o = U_L A (T_{col} - T_a)$$

The higher the temperature difference between collector temperature and ambient temperature, the higher the heat loss. U_L is overall heat transfer coefficient.

The useful energy extracted by collector can be expressed as

$$Q_u = Q_i - Q_o = I \tau \alpha \cdot A - U_L A (T_{col} - T_a)$$

The amount of heat received by the heat transfer fluid in absorber tube can be measured by

$$Q_u = \dot{m} c_p (T_o - T_i)$$

Since the temperature of collector is difficult to measured, heat removal factor is introduced.

Heat removal factor can be related to the actual useful heat gain to useful heat gain if the surface of collector temperature is same as inlet temperature.

$$F_R = \frac{\dot{m} c_p (T_o - T_i)}{A [I \tau \alpha - U_L (T_i - T_o)]}$$

The actual useful energy gain can be written as

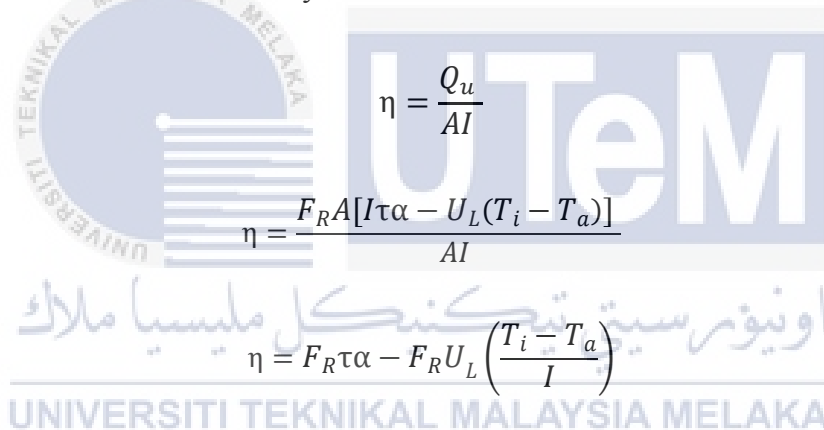
$$Q_u = F_R A [I \tau \alpha - U_L (T_i - T_a)]$$

This equation is known as “Hottel-Whillier-Bliss equation (Struckmann, 2008).

The Hottel-Whillier_Bliss equation is applied to calculate the thermal efficiency. The thermal efficiency of thermal collector is:

$$\eta = \frac{\int Q_u dt}{A \int I dt}$$

The instantaneous thermal efficiency is:



$$\eta = \frac{Q_u}{AI}$$

$$\eta = \frac{F_R A [I \tau \alpha - U_L (T_i - T_a)]}{AI}$$

$$\eta = F_R \tau \alpha - F_R U_L \left(\frac{T_i - T_a}{I} \right)$$

2.3 Photovoltaic Thermal Hybrid Solar Collector

Photovoltaic thermal hybrid solar collector, also known as PV/T or PVT is a system that combines photovoltaic panel and solar thermal collector. Hence, it can convert solar radiation into electrical and thermal energy simultaneously. The photovoltaic panel is placed on top of thermal collector and converts sunlight into electrical energy. However, the sunlight brings along the heat which will affect the performance of photovoltaic panel. The underneath thermal collector helps to extract the heat energy from photovoltaic panel by the

heat transfer fluid. At the moment, heat transfer fluid gained heat energy which can be utilized for water heating or space heating.

PVT collector consists of glazing cover, photovoltaic cell, backsheet layer, absorber plate, tube, insulation (Figure 2.5). The insulation is placed under absorber or surrounded absorber to prevent the heat loss and ensure the temperature of the system is uniform (Khelifa, Touafek, Ben Moussa, & Tabet, 2016).

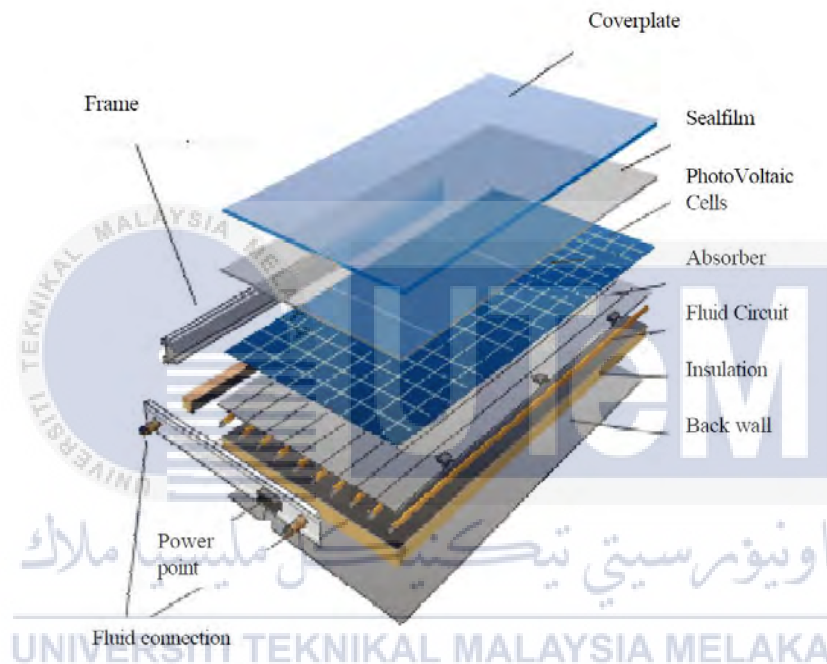


Figure 2.5 Main Components of PVT Collector

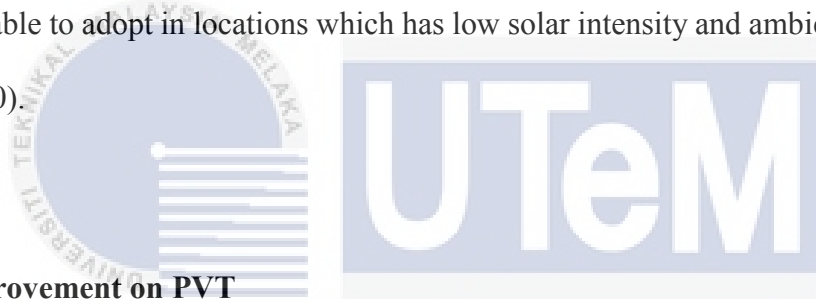
2.3.1 Photovoltaic Thermal Solar Water Collector

The photovoltaic thermal solar water collector is also known as PVT/w collector. Thermal efficiency of PVT/w collector for unglazed and glazed is between 45 – 70% (Chow, 2010). Water is more effective than air as PVT/w has higher electric output. For the location with high level of solar radiation, PVT/w is useful as it can help in water pre-heating and space heating. PVT/w collector has more restriction on system design and operation because PVT/w require a heat exchanger material which his good thermal contact with the PV rear

surface (Tripanagnostopoulos, 2007). However, thermal efficiency of PVT/w collector is higher than PVT/a due to the higher density of water.

2.3.2 Photovoltaic Thermal Solar Air Collector

Photovoltaic thermal solar air collector can be written as PVT/a collector. Thermal efficiency of PVT/a collector can reach 55% for optimized collector design (Chow, 2010). The PVT/a collector uses natural or forced flow of air for PV cooling and space heating. The forced flow has better conduction and convection effect, therefore will be more effective but requires electricity to power the external device, compared to natural flow. PVT/a collector is more suitable to adopt in locations which has low solar intensity and ambient temperature (Chow, 2010).



2.4 Improvement on PVT

Since the 1970s, a large amount of effect is invested on the development of photovoltaic thermal technology. Theoretical model and important design parameter are identified for the improvement of PVT technology. Many researches have been done on innovation of design of absorber and concentrated PVT collector

2.4.1 Application of New Design of Absorber

Changing PVT design of absorber is the one of the methods to improve the total efficiency of PVT. There were several experimental and simulation studies conducted to identify the total efficiency of PVT with different design of absorber (Ibrahim et al., 2009).

2.4.2 Application of Concentrator

By installing the concentrator on photovoltaic thermal collector, sunlight can be focused on the photovoltaic thermal collector receiver. The combination of the system can be called as concentrated photovoltaic thermal collector or CPVT. Concentrated photovoltaic thermal collector utilize the refraction of lenses or reflection of lenses mechanism to focus the sunlight on the receiver of PVT. CPVT has lower cost per unit area than a normal flat plate PVT.



2.5 Comparison of Study

Table 2.2 shows a summarized comparison of the absorber design, thermal, electrical and total efficiency of PVT.

Table 2.2 Comparison of Study

Researcher(s)	Method	Parameter	$\eta_{th}, \%$	$\eta_{el}, \%$	$\eta_{Total}, \%$
Adnan Ibrahim, Ahmad Fudholi, Kamaruzzaman Sopian, Mohd Yusof Othman, Mohd Hafidz Ruslan (2014)	Experiment	Spiral design absorber Rectangular tube $\dot{m} = 0.027 \text{ kg/s}$	48	10.8	58.8
Jie Ji, Jian-Ping Lu, Tin-Tai Chow, Wei He, Gang Pei (2007)	Experiment	Harp design absorber Batten tube $m/A_c = 80 \text{ kg/m}^2$	45	10.15	55.15
B. J. Huang, T. H. Lin, W. C. Hung and F. S. Sun (2001)	Experiment	Harp design absorber Round tube $V/A_c = 82 \text{ l/m}^2$	38	9	47
James Allan, Zahir Dehouche, Sinisa Stankovic and Lascelle Mauricette (2015)	Simulation	Serpentine design absorber $\dot{m} = 0.009 \text{ kg/s}$	54.54	7.46	62
Charles D. Corbin, Zhiqiang John Zhai (2010)	Simulation, CFD	Harp design absorber Round tube $v = 0.345 \text{ m/s}$	29.6	5.3	34.9

CHAPTER 3

METHODOLOGY

3.1 Introduction

In this chapter, the methodology used to obtain the outlet temperature of heat transfer fluid and temperature of photovoltaic panel of PVT is shown. The numerical simulation will be carried out by using Fluent in ANSYS Workbench. After the results from Fluent is obtained, mathematics calculation is applied to calculate the thermal efficiency, electrical efficiency and total efficiency of PVT.

The simulation starts with the geometry drawing. There are two options to obtain the geometry in FLUENT, first the use of Design Modeler in ANSYS workbench, second is importing the geometry which is drawn in CAD software, such as CATIA and Solidworks. ANSYS Meshing is used to generate mesh for the geometry. After the completion of meshing, the model for CFD simulation is set up in Fluent. The results obtained from the simulation will be used to calculate the performance of PVT by using formula. A flow chart of methodology is shown in Figure 3.1.

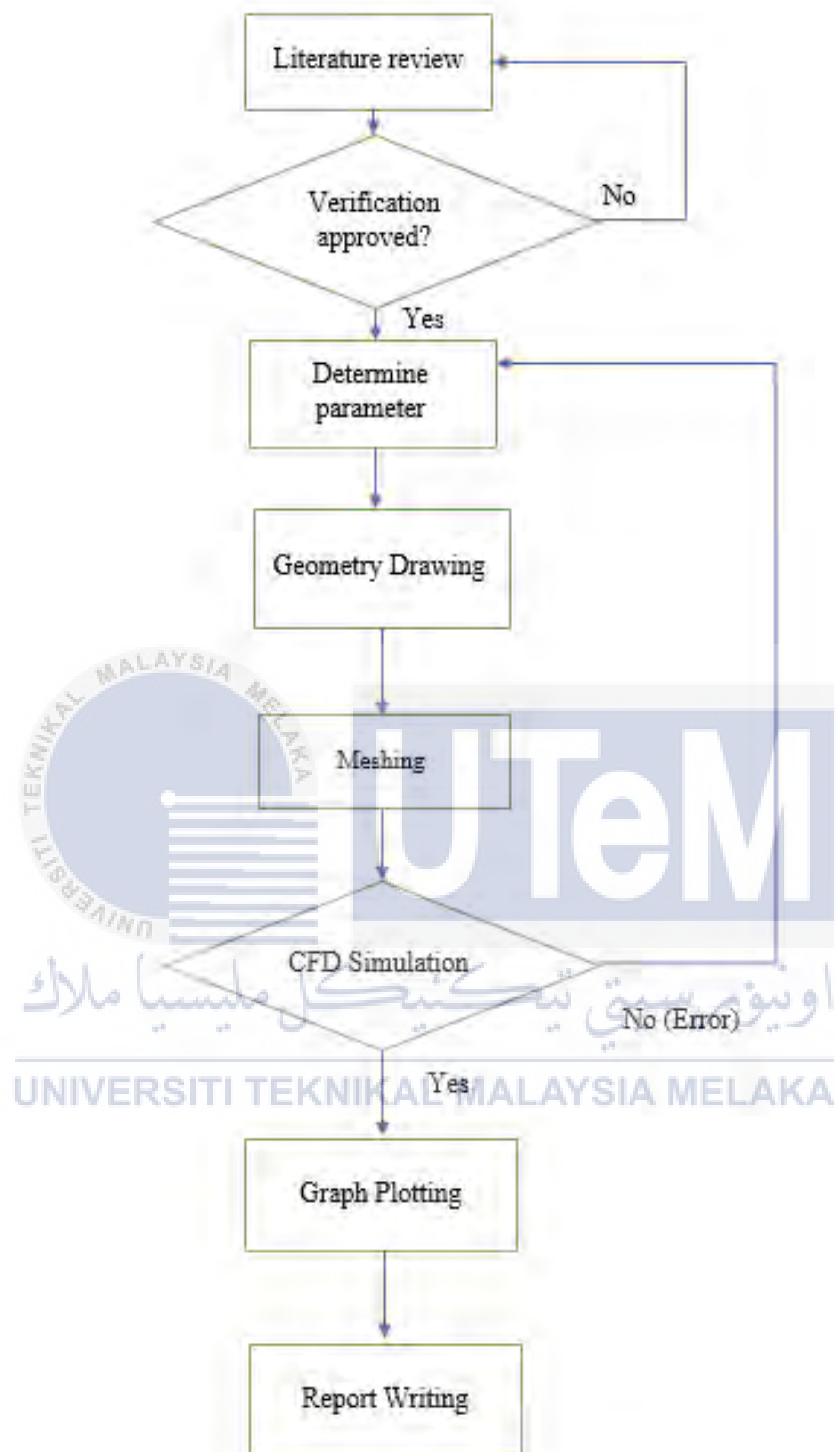


Figure 3.1 Flow chart of the Methodology

3.2 Geometry Drawing

Every components of PVT are drawn one by one in CATIA Part Design. CATIA Assembly Design is utilized to assemble all the components of PVT. The components of PVT comprised of top cover, encapsulant of photovoltaic panel, photovoltaic panel, backsheet, thermal paste and absorber. Horizontal serpentine absorber, vertical serpentine absorber and spiral absorber is designed and drawn in CATIA as shown in Figure 3.2, Figure 3.3 and Figure 3.4 respectively. Cross-section of absorber is illustrated in Figure 3.5, the values in Figure 3.5 are in unit of millimeter. Length of every absorber are the same, which is 4.8m. Table 3.1 shows the dimension of PVT components. The arrangement of PVT is shown in Figure 3.6. There is no absorber plate is attached to absorber tube as this design without absorber plate is found to perform well in thermal efficiency. Thus, the extra absorber plate may increases the weight and manufacturing cost of PVT (Nahar, Hasanuzzaman, & Rahim, 2017).

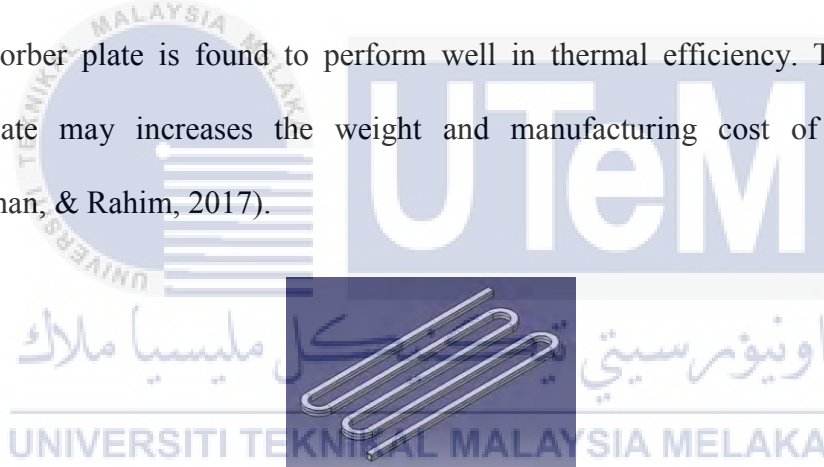


Figure 3.2 Horizontal Serpentine Absorber in CATIA Part Design

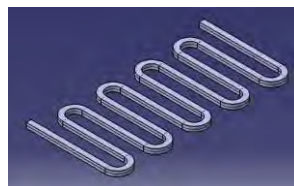


Figure 3.3 Vertical Serpentine Absorber in CATIA Part Design

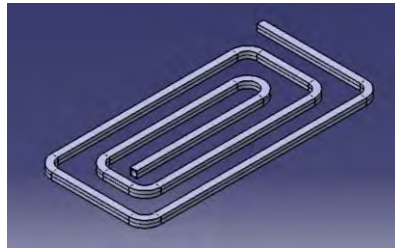


Figure 3.4 Spiral Absorber in CATIA Part Design

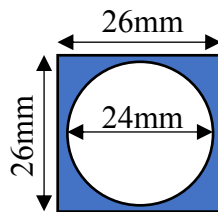


Figure 3.5 Cross-section of Absorber

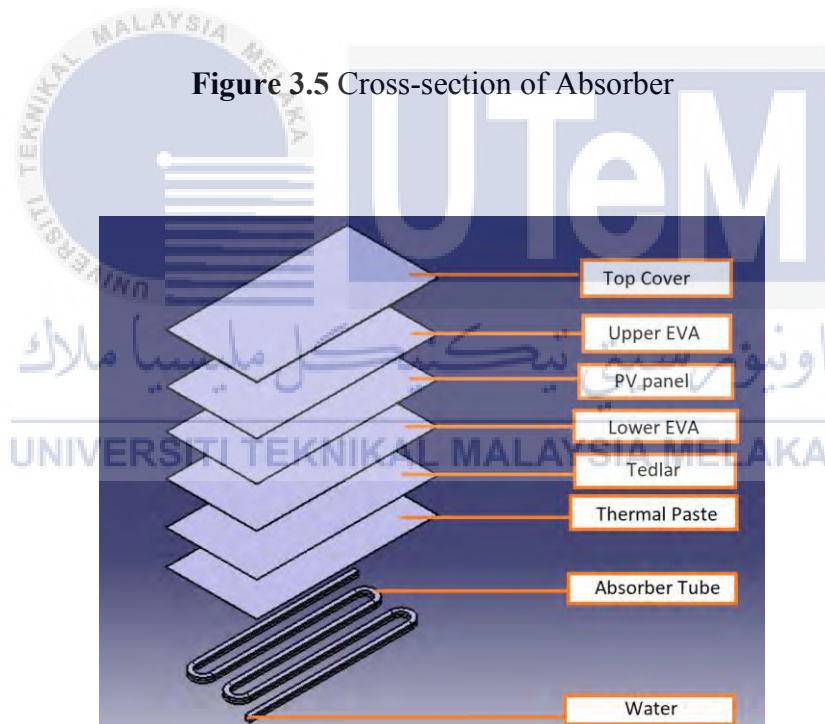


Figure 3.6 Exploded View of PVT

Table 3.1 Dimension of PVT Components

PVT Components	Dimensions (m^3)
Top cover	1.0 x 0.5 x 0.003
Encapsulant of PV	1.0 x 0.5 x 0.0008
PV panel	1.0 x 0.5 x 0.0001
Backsheet	1.0 x 0.5 x 0.00005
Thermal Paste	1.0 x 0.5 x 0.0003

3.3 Meshing

Meshing can be defined as a process to divide a geometry into number of elements and nodes. Therefore, when load is applied on the geometry, the load can be distributed uniformly on the geometry. The more the elements and nodes, which means the smaller the elements, the more accurate the results but more time consuming. However, too few of elements will lead to inaccurate results (Khelifa, Touafek, Ben Moussa, & Tabet, 2016). In the simulation in this study, “Fine” is chose for the relevance center and “High” is selected for smoothing in sizing section. The meshing elements are mainly made up of tetrahedral and hexahedral elements.

3.4 Pre-processing

The double precision option is activated to obtain the more accurate results. The energy equation is enabled to allow the calculation of heat transfer. Laminar flow model is used for the simulations since Reynolds number of heat transfer fluid flow is less than 2300. For the radiation model, surface-to-surface (S2S) model is applied. S2S radiation model assumes the surfaces are gray and diffuse surfaces. Thus, the model is not involved in absorption, emission, and scattering of radiation, only “surface to surface” radiation is accounted. Sun direction vector is used to determine the direction of solar irradiation. In the simulation of this study, the direction of solar irradiance is irradiated perpendicularly to the surface of the glass cover. The materials of every components of PVT and its properties are shown in Table 3.1. Length of absorber tube are same, which is 4.8m. Water is selected as the heat transfer fluid. The mass flow rate of inlet flow is varied from 0.0005kg/s to 0.005kg/s. Inlet temperature is 27°C.

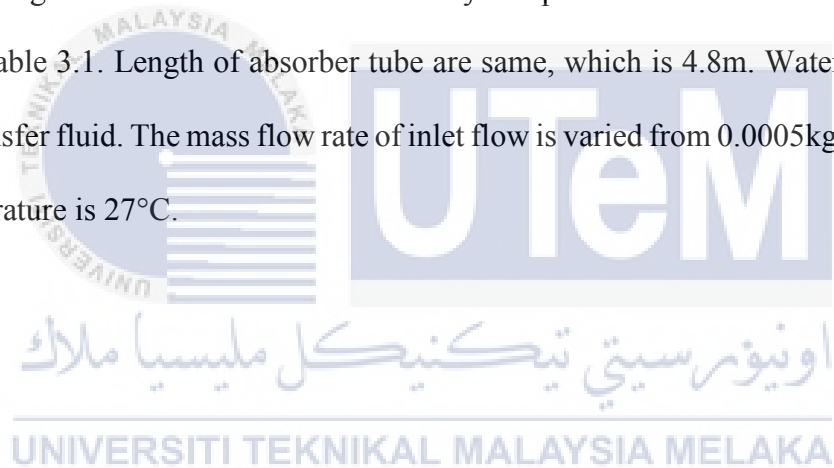


Table 3.2 Material Properties of PVT Components (Nahar et al., 2017)

Components of PVT	Material	Density (kg/m^3)	Specific Heat Capacity (J/kg.K)	Thermal Conductivity (W/m.K)
Top cover	Glass	2450	500	2
Encapsulant of PV	EVA (Ethylene-vinyl-acetate)	950	2090	0.311
PV panel	Silicon	2329	700	148
Backsheet	Tedlar/PVF (Polyvinyl fluoride)	1200	1250	0.15
Thermal Paste	Conductor	2600	700	1.9
Absorber	Aluminium	2700	900	160
Heat transfer fluid	Water	998.2	4182	0.6

3.5 Post-processing

Contour diagrams can be plotted after the numerical calculation is completed. Temperature is the variable that is taken into account in the contour diagrams. From the contour diagrams, temperature of every spot on the selected surface can be reviewed. Besides that, average temperature on the surface of outlet and PV panel is also required to obtain for the calculation of thermal efficiency and electrical efficiency.

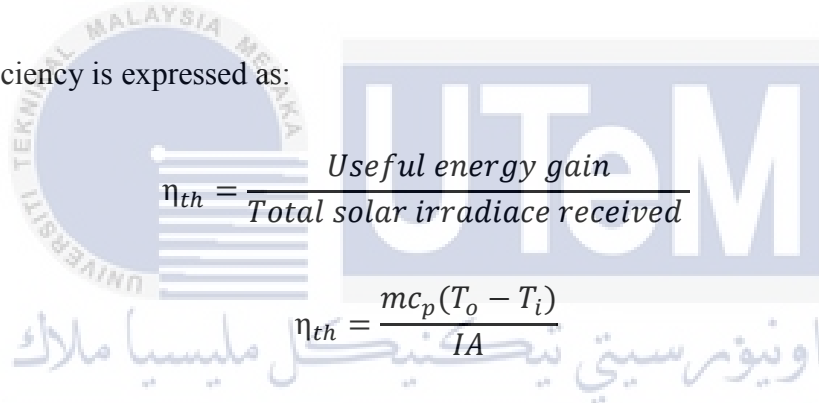
3.6 Mathematics Calculation

PV efficiency is expressed as:

$$\eta_{pv} = \eta_{ref} [1 - \beta_{ref}(T_c - T_{ref})]$$

where η_r represents reference efficiency of PV panel, β_{ref} represents temperature coefficient, T_c represents PV cell temperature and T_{ref} is reference temperature (Skoplaki & Palyvos, 2009). For $T_{ref} = 25^\circ\text{C}$, the η_{ref} and β_{ref} of silicon-based PV panel are about $0.0045^\circ\text{C}^{-1}$ and 0.12 respectively (Skoplaki & Palyvos, 2009). By using this formula, the PV temperature obtained from simulation can be used to calculate the PV efficiency since η_{ref} , β_{ref} and T_{ref} are constant.

Thermal efficiency is expressed as:


$$\eta_{th} = \frac{\text{Useful energy gain}}{\text{Total solar irradiance received}}$$
$$\eta_{th} = \frac{mc_p(T_o - T_i)}{IA}$$

where m is mass flow rate, c_p is specific heat capacity of heat transfer fluid, T_o is outlet temperature, T_i is inlet temperature, I is solar irradiance intensity and A is area of collector.

Total efficiency, η_{Total} is sum of the thermal efficiency and PV efficiency (Ibrahim et al., 2009).

$$\eta_{Total} = \eta_{pv} + \eta_{th}$$

3.7 Validation

Validation was conducted by referring to the previous research (Senthil Kumar et al., 2015). The coordinates of location used in simulation was set at India. There were two comparisons in this validation, first was compared to previous research simulation results, second was compared to experimental results.

From Figure 3.7, it shows the experimental and simulation results from 8a.m. to 5p.m. on a specific day of April. The difference of the outlet temperature between current and previous research simulation results varied from 0% to 9.33%. The highest percentage difference was 9.33% and root mean square error is only 2.52°C. The root mean square error between previous research simulation and previous experimental results is 2.08°C. The difference of the outlet temperature between current research simulation results and previous research experimental results varied from 0.22% to 6.89%. The highest percentage error was 6.89% and root mean square error is 1.29°C, which is lower than root mean square error between previous research simulation and previous experimental results. Hence, this method is validated and assumed as applicable to case in this study.

UNIVERSITI TEKNIKAL MALAYSIA MELAKA

Table 3.3 Comparison of Results for Validation

Time (Hours)	Experimental Inlet Air Temperature, T_i (°C)	Experimental Outlet Air Temperature, T_o (°C)	Paper Simulation Outlet Air Temperature, T_o (°C)	Current Simulation Outlet Air Temperature, T_o (°C)
8	34.5	36	35	36.5
9	38	40	37	41.2
10	41	44	41	44.8
11	42	46	44	46.1
12	42	47	46	46.2
1	45	49.5	47	49.3
2	43	44	44	47.03
3	37	43	41	42.06
4	37	42	39	41.62
5	36	38	38	39.58

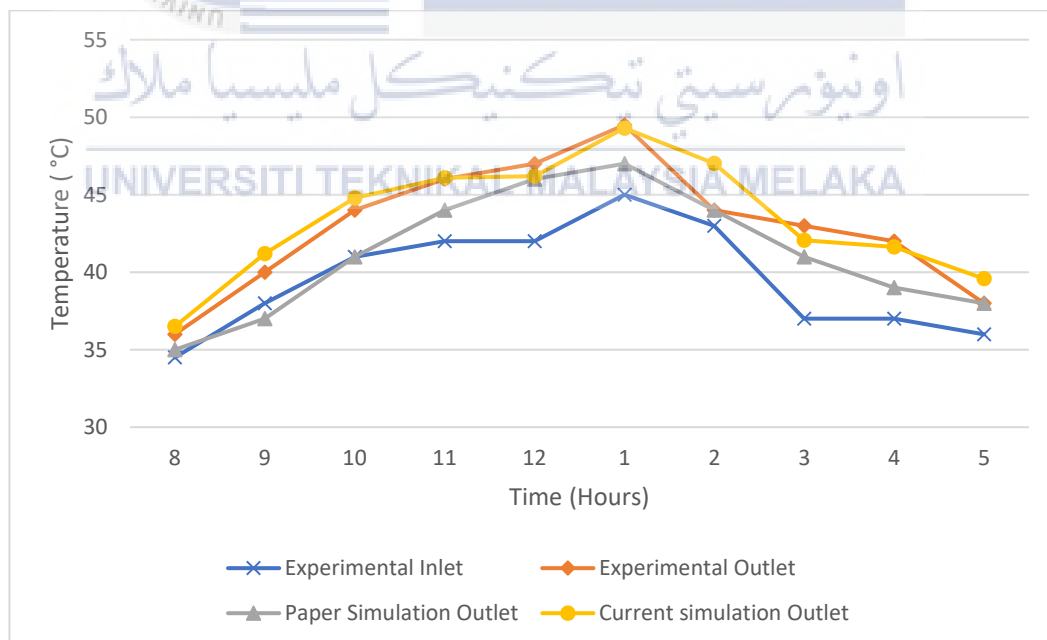


Figure 3.7 Changes in Outlet Temperature with Time

CHAPTER 4

RESULTS AND DISCUSSION

4.1 Influence of Mass Flow Rate on Thermal Efficiency

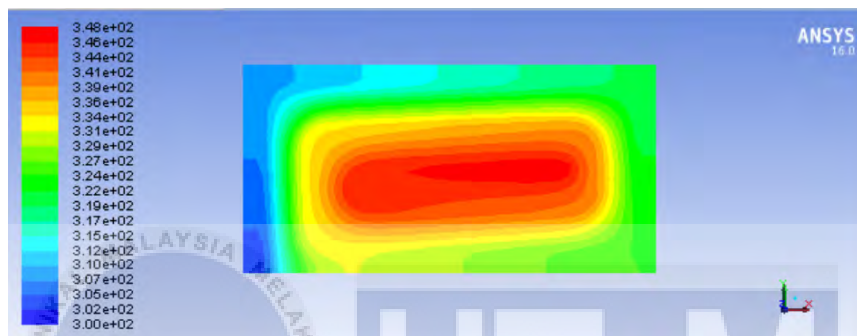


Figure 4.1 Contour Diagram of PV of spiral absorber PVT at 0.0005 kg/s under $1000W/m^2$ solar irradiance



Figure 4.2 Contour Diagram of water surface of spiral absorber PVT at 0.0005 kg/s under $1000W/m^2$ solar irradiance

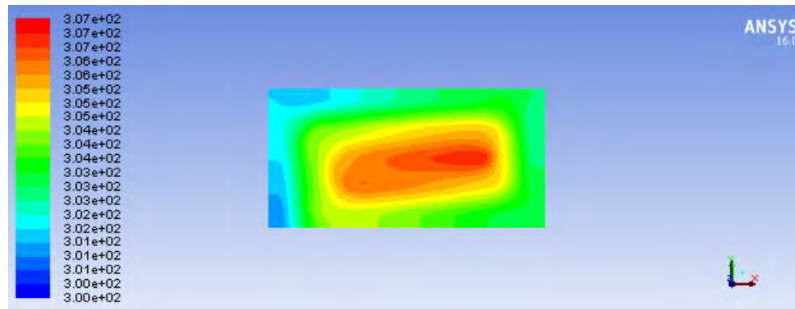


Figure 4.3 Contour Diagram of PV of spiral absorber PVT at 0.005 kg/s under $1000W/m^2$ solar irradiance

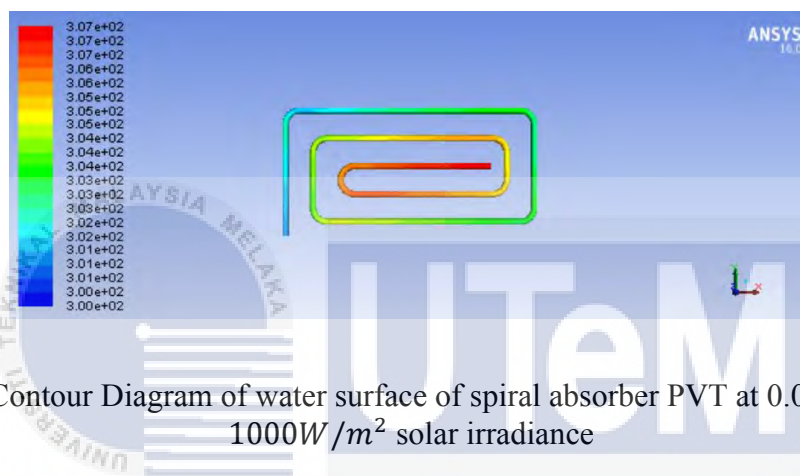


Figure 4.4 Contour Diagram of water surface of spiral absorber PVT at 0.005 kg/s under $1000W/m^2$ solar irradiance

Figure 4.1 and 4.2 shows temperature contour diagram of PV surface and water surface of spiral absorber PVT at 0.0005 kg/s under $1000W/m^2$ solar irradiance while Figure 4.3 and 4.3 shows temperature contour diagram of PV surface and water surface of spiral absorber PVT at 0.005 kg/s under $1000W/m^2$ solar irradiance. From the Figure 4.1 – 4.4, at 0.0005kg/s mass flow rate, the temperature is relatively higher as compared to the case of 0.005kg/s. According to the heat transfer formula,

$$\frac{Q}{t} = \dot{m} \cdot c \cdot \Delta T$$

mass flow rate is inversely proportional to temperature difference between initial temperature and final temperature. Therefore, the higher the mass flow rate, the lower the temperature difference. Since the inlet temperature in this study was constant, thus the higher

the mass flow rate, the lower the outlet temperature. As the mass flow rate increased, the duration for heat transfer is reduced, hence outlet temperature is lower.

Mass flow rate and temperature difference are the variables to determine the thermal efficiency. Figure 4.1, 4.2 and 4.3 are illustrated the changes in temperature difference and thermal efficiency with mass flow rate from 0.0005 kg/s to 0.005 kg/s under $1000W/m^2$, $800W/m^2$ and $600W/m^2$ solar irradiance respectively.

Table 4.1 Results of Outlet Temperature and Thermal Efficiency of Horizontal Serpentine Absorber under $1000W/m^2$ Solar Irradiance

Mass Flow Rate, \dot{m} (kg/s)	Outlet Temperature, T_o (°C)	Temperature Difference, ΔT (°C)	Thermal Efficiency, η_{th} (%)
0.0005	72.74	45.74	19.13
0.00075	59.90	32.90	20.64
0.001	52.08	25.08	20.98
0.002	39.95	12.95	21.66
0.003	35.80	8.80	22.08
0.004	33.69	6.69	22.38
0.005	32.41	5.41	22.62

Table 4.2 Results of Outlet Temperature and Thermal Efficiency of Vertical Serpentine Absorber under $1000\text{W}/\text{m}^2$ Solar Irradiance

Mass Flow Rate, \dot{m} (kg/s)	Outlet Temperature, T_o ($^{\circ}\text{C}$)	Temperature Difference, ΔT ($^{\circ}\text{C}$)	Thermal Efficiency, η_{th} (%)
0.0005	74.09	47.09	19.69
0.00075	60.73	33.73	21.16
0.001	52.63	25.63	21.44
0.002	40.14	13.14	21.98
0.003	35.87	8.87	22.26
0.004	33.70	6.70	22.42
0.005	32.39	5.39	22.54

Table 4.3 Results of Outlet Temperature and Thermal Efficiency of Spiral Absorber under $1000\text{W}/\text{m}^2$ Solar Irradiance

Mass Flow Rate, \dot{m} (kg/s)	Outlet Temperature, T_o ($^{\circ}\text{C}$)	Temperature Difference, ΔT ($^{\circ}\text{C}$)	Thermal Efficiency, η_{th} (%)
0.0005	74.20	47.20	19.74
0.00075	61.23	34.23	21.47
0.001	53.04	26.04	21.78
0.002	40.35	13.35	22.33
0.003	36.03	9.03	22.66
0.004	33.83	6.83	22.85
0.005	32.49	5.49	22.96

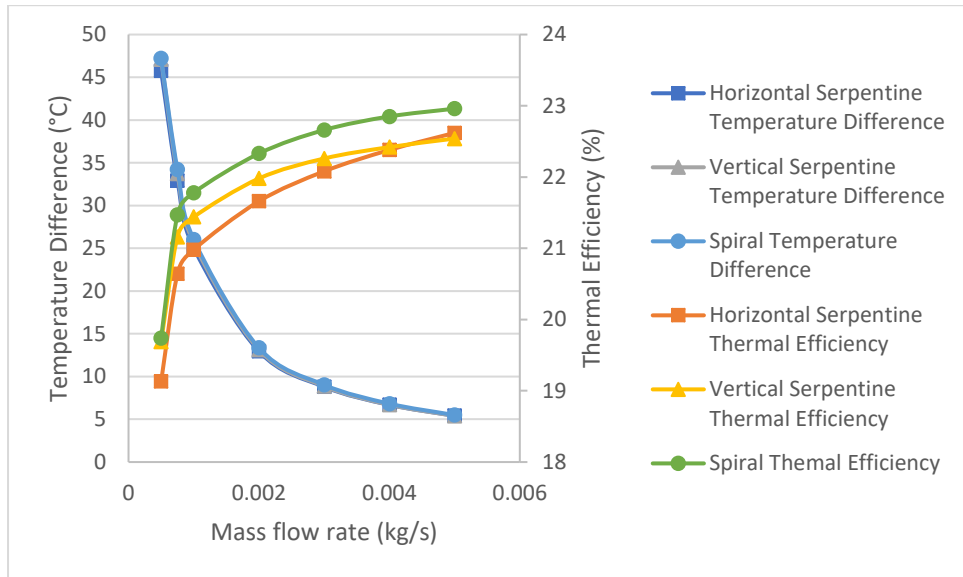


Figure 4.5 Changes in Temperature Difference and Thermal Efficiency with Various Mass Flow Rate under $1000W/m^2$ Solar Irradiance

Based on Figure 4.5, under $1000W/m^2$ solar irradiance, the highest temperature differences between inlet and outlet is achieved at 0.0005 kg/s . At 0.0005 kg/s , spiral absorber obtained 47.20°C temperature difference and followed by vertical serpentine absorber and horizontal serpentine absorber which had 47.09°C and 45.74°C temperature difference respectively. Hence, spiral absorber had the highest thermal efficiency, 19.74% at 0.0005 kg/s .

As the mass flow rate increased, the temperature difference decreased but thermal efficiencies were increased. This proved that the effect of mass flow rate is override the effect of temperature difference. The highest thermal efficiencies were achieved at 0.005kg/s . At 0.005kg/s , spiral absorber had highest thermal efficiency, 22.96% and followed by horizontal serpentine absorber and vertical serpentine absorber with 22.62% and 22.54% .

The increase rate of thermal efficiency is lower at higher mass flow rate. Thermal efficiency of spiral absorber was leading from 0.0005kg/s to 0.005kg/s . Thermal efficiency

of horizontal serpentine absorber is lowest at lower mass flow rate. However, as the mass flow rate increased, the difference of thermal efficiency between horizontal serpentine and vertical serpentine was became smaller. Until 0.005kg/s, thermal efficiency of horizontal serpentine absorber started to surpass thermal efficiency of vertical serpentine.

Table 4.4 Results of Outlet Temperature and Thermal Efficiency of Horizontal Serpentine Absorber under 800W/m² Solar Irradiance

Mass Flow Rate, \dot{m} (kg/s)	Outlet Temperature, T_o (°C)	Temperature Difference, ΔT (°C)	Thermal Efficiency, η_{th} (%)
0.0005	62.96	35.96	18.80
0.00075	52.71	25.71	20.16
0.001	46.58	19.58	20.47
0.002	37.10	10.10	21.12
0.003	33.86	6.86	21.52
0.004	32.22	5.22	21.83
0.005	31.22	4.22	22.06

UNIVERSITI TEKNIKAL MALAYSIA MELAKA

Table 4.5 Results of Outlet Temperature and Thermal Efficiency of Vertical Serpentine Absorber under 800W/m² Solar Irradiance

Mass Flow Rate, \dot{m} (kg/s)	Outlet Temperature, T_o (°C)	Temperature Difference, ΔT (°C)	Thermal Efficiency, η_{th} (%)
0.0005	64.18	37.18	19.44
0.00075	53.48	26.48	20.76
0.001	47.11	20.11	21.03
0.002	37.30	10.30	21.54
0.003	33.96	6.96	21.83
0.004	32.26	5.26	22.00
0.005	31.22	4.22	22.06

Table 4.6 Results of Outlet Temperature and Thermal Efficiency of Spiral Absorber under 800W/m² Solar Irradiance

Mass Flow Rate, \dot{m} (kg/s)	Outlet Temperature, T_o (°C)	Temperature Difference, ΔT (°C)	Thermal Efficiency, η_{th} (%)
0.0005	64.46	37.46	19.58
0.00075	53.99	26.99	21.16
0.001	47.52	20.52	21.45
0.002	37.51	10.51	21.98
0.003	34.11	7.11	22.30
0.004	32.38	5.38	22.50
0.005	31.33	4.33	22.64

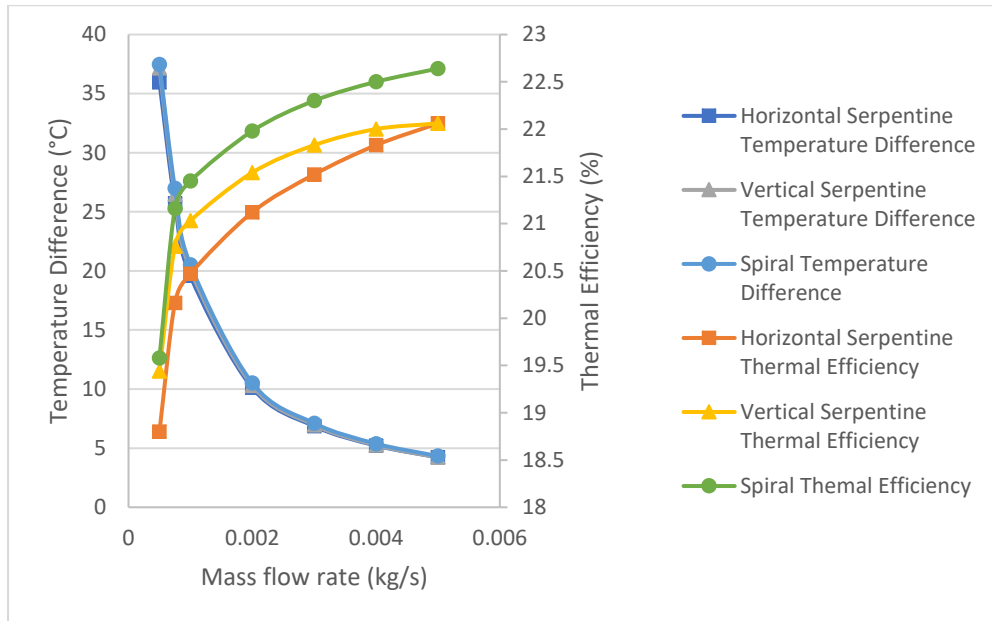


Figure 4.6 Changes in Temperature Difference and Thermal Efficiency with Various Mass Flow Rate under $800W/m^2$ Solar Irradiance

Based on Figure 4.6, under $800W/m^2$ solar irradiance, the trend of the changes in temperature difference and thermal efficiency were same as in $1000W/m^2$ solar irradiance. The highest thermal efficiency was achieved at $0.005kg/s$. At $0.005kg/s$, spiral absorber was higher by 0.58% than horizontal serpentine and vertical serpentine absorber since thermal efficiency of both were the same, which were 22.06%.

Table 4.7 Results of Outlet Temperature and Thermal Efficiency of Horizontal Serpentine Absorber under 600W/m² Solar Irradiance

Mass Flow Rate, \dot{m} (kg/s)	Outlet Temperature, T_o (°C)	Temperature Difference, ΔT (°C)	Thermal Efficiency, η_{th} (%)
0.0005	53.01	26.01	18.13
0.00075	45.50	18.50	19.34
0.001	41.08	14.08	19.63
0.002	34.26	7.26	20.24
0.003	31.93	4.93	20.62
0.004	30.75	3.75	20.91
0.005	30.03	3.03	21.12

Table 4.8 Results of Outlet Temperature and Thermal Efficiency of Vertical Serpentine Absorber under 600W/m² Solar Irradiance

Mass Flow Rate, \dot{m} (kg/s)	Outlet Temperature, T_o (°C)	Temperature Difference, ΔT (°C)	Thermal Efficiency, η_{th} (%)
0.0005	54.13	27.13	18.91
0.00075	46.21	19.21	20.08
0.001	41.58	14.58	20.32
0.002	34.47	7.47	20.83
0.003	32.04	5.04	21.08
0.004	30.81	3.81	21.24
0.005	30.06	3.06	21.32

Table 4.9 Results of Outlet Temperature and Thermal Efficiency of Spiral Absorber under $600W/m^2$ Solar Irradiance

Mass Flow Rate, \dot{m} (kg/s)	Outlet Temperature, T_o (°C)	Temperature Difference, ΔT (°C)	Thermal Efficiency, η_{th} (%)
0.0005	54.45	27.56	19.21
0.00075	46.73	19.73	20.63
0.001	41.99	14.99	20.90
0.002	34.68	7.68	21.41
0.003	32.19	5.19	21.70
0.004	30.93	3.93	21.91
0.005	30.16	3.16	22.03

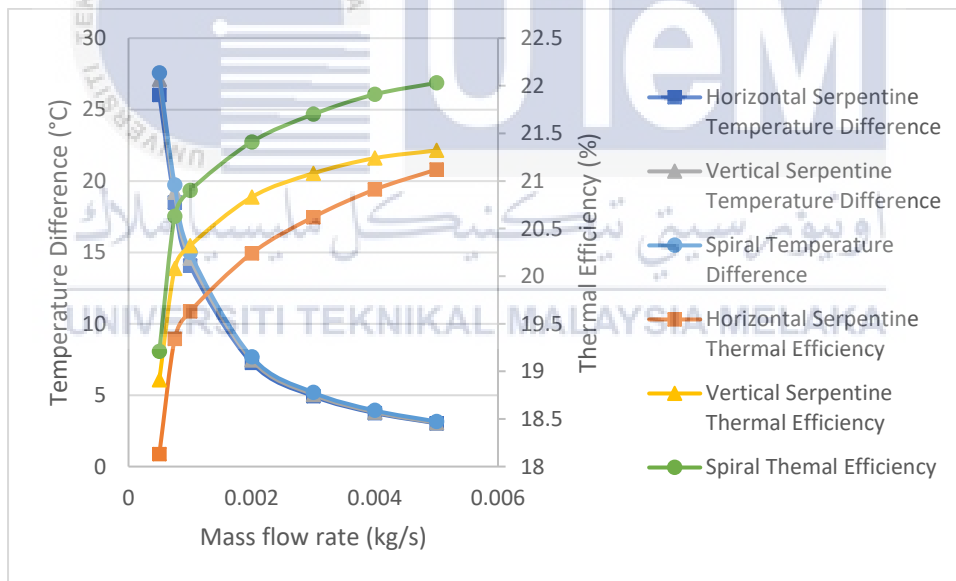


Figure 4.7 Changes in Temperature Difference and Thermal Efficiency with Various Mass Flow Rate under $600W/m^2$ Solar Irradiance

Based on Figure 4.7, under $600W/m^2$ solar irradiance, the trend of the changes in temperature difference and thermal efficiency were same as in $1000W/m^2$ and $800W/m^2$ solar irradiance. The highest thermal efficiency was achieved at $0.005kg/s$. At $0.005kg/s$, spiral absorber was higher by 0.71% as compared to vertical serpentine absorber and by 0.91% as compared to vertical serpentine absorber.

4.2 Influence of Mass Flow Rate on Photovoltaic Panel Efficiency

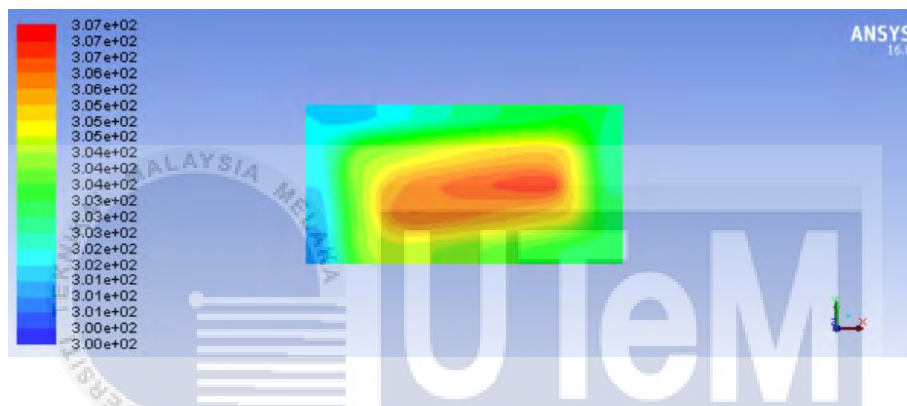


Figure 4.8 Contour Diagram of PV of spiral absorber PVT at 0.005 kg/s under $1000W/m^2$ solar irradiance

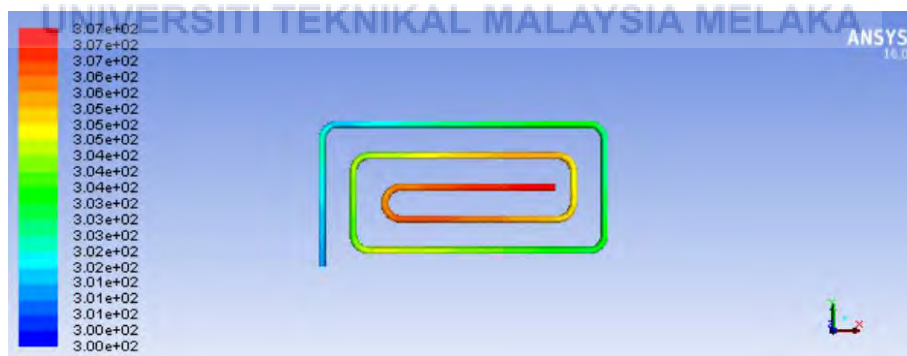


Figure 4.9 Contour Diagram of water surface of spiral absorber PVT at 0.005 kg/s under $1000W/m^2$ solar irradiance

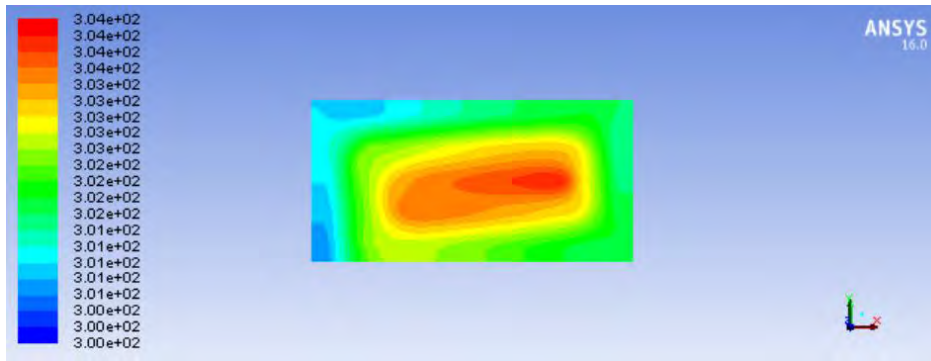


Figure 4.10 Contour Diagram of PV of spiral absorber PVT at 0.005 kg/s under $600W/m^2$ solar irradiance

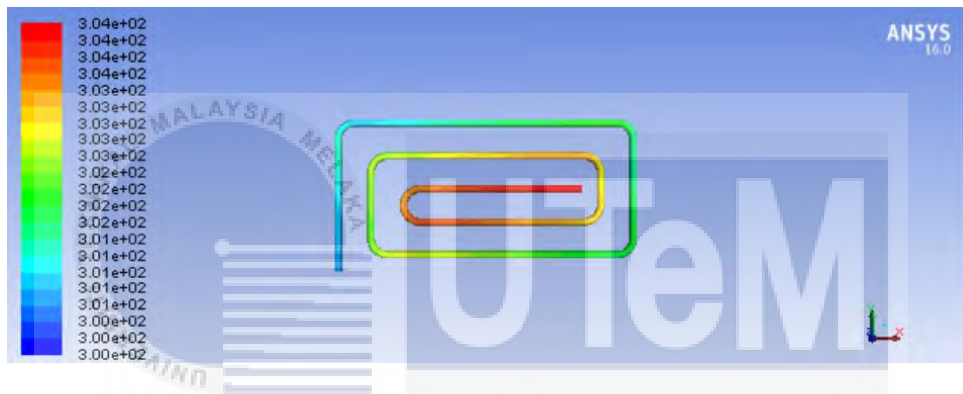


Figure 4.11 Contour Diagram of PV of spiral absorber PVT at 0.005 kg/s under $600W/m^2$ solar irradiance

UNIVERSITI TEKNIKAL MALAYSIA MELAKA

Figure 4.8 and 4.9 shows the temperature contour diagram of PV surface and water surface of spiral absorber at 0.005 kg/s under $1000W/m^2$ solar irradiance while Figure 4.10 and 4.11 shows the temperature contour diagram of PV surface and water surface of spiral absorber at 0.005 kg/s under $600W/m^2$ solar irradiance. From the Figure 4.8 – 4.11, the temperature of PVT under $600W/m^2$ solar irradiance is slightly lower. According to general definition of heat transfer coefficient,

$$h = \frac{q}{\Delta T}$$

the heat flux, q is directly proportional to temperature difference, ΔT . Hence, as the solar irradiance intensity decreased, the temperature difference also increased. Since inlet temperature was constant in this study, therefore the higher the solar irradiance intensity, the higher outlet temperature.

Figure 4.12, 4.13 and 4.14 show the changes in PV temperature with various mass flow rate. The PV temperature is directly proportional to PV efficiency. PV temperature is the only variable to determine PV efficiency. PV panel has a characteristic which is it will perform at low efficiency in high temperature and vice versa. Figures 4.12, 4.13 and 4.14 also illustrate a decrease in PV temperature as result of the increased in mass flow rate.

Table 4.10 Results of PV Temperature and PV Efficiency of Horizontal Serpentine Absorber under $1000\text{W}/\text{m}^2$ Solar Irradiance

Mass Flow Rate, \dot{m} (kg/s)	PV Temperature, T_c ($^{\circ}\text{C}$)	Electrical Efficiency, η_{pv} (%)
0	65.27	9.83
0.0005	54.23	10.42
0.00075	46.29	10.85
0.001	41.93	11.09
0.002	35.33	11.44
0.003	33.07	11.56
0.004	31.88	11.63
0.005	31.14	11.67

Table 4.11 Results of PV Temperature and PV Efficiency of Vertical Serpentine Absorber under 1000W/m² Solar Irradiance

Mass Flow Rate, \dot{m} (kg/s)	PV Temperature, T_c (°C)	Electrical Efficiency, η_{pv} (%)
0	65.99	9.79
0.0005	54.03	10.43
0.00075	46.09	10.86
0.001	41.70	11.10
0.002	35.07	11.46
0.003	32.78	11.58
0.004	31.59	11.64
0.005	30.85	11.68

Table 4.12 Results of PV Temperature and PV Efficiency of Spiral Absorber under 1000W/m² Solar Irradiance

Mass Flow Rate, \dot{m} (kg/s)	PV Temperature, T_c (°C)	Electrical Efficiency, η_{pv} (%)
0	66.48	9.76
0.0005	56.21	10.31
0.00075	47.53	10.78
0.001	42.67	11.05
0.002	35.44	11.44
0.003	33.04	11.57
0.004	31.82	11.63
0.005	31.07	11.67

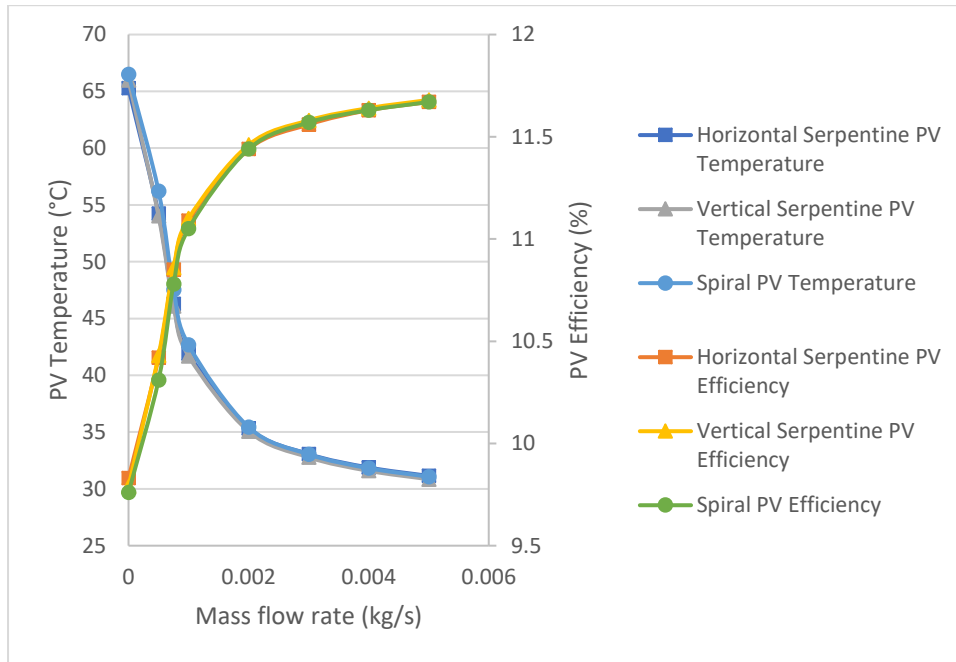


Figure 4.12 Changes in PV Temperature and PV Efficiency with Various Mass Flow Rate under $1000W/m^2$ Solar Irradiance

Based on Figure 4.12, the higher the mass flow rate, the lower the PV temperature, hence the PV efficiency was higher. The trend of increase rate of PV efficiency was similar to the trend of thermal efficiency. As the mass flow rate increased, the increase rate of PV efficiency was become lower. PV efficiency did not show significant difference among the three different design of absorber tube, especially at higher mass flow rate. At 0.005kg/s mass flow rate, horizontal serpentine and spiral absorber achieved 11.67% while vertical serpentine achieved 11.68%.

Table 4.13 Results of PV Temperature and PV Efficiency of Horizontal Serpentine Absorber under 800W/m² Solar Irradiance

Mass Flow Rate, \dot{m} (kg/s)	PV Temperature, T_c (°C)	Electrical Efficiency, η_{pv} (%)
0	58.14	10.21
0.0005	48.33	10.74
0.00075	42.07	11.08
0.001	38.65	11.26
0.002	33.50	11.54
0.003	31.74	11.64
0.004	30.81	11.69
0.005	30.23	11.72

Table 4.14 Results of PV Temperature and PV Efficiency of Vertical Serpentine Absorber under 800W/m² Solar Irradiance

Mass Flow Rate, \dot{m} (kg/s)	PV Temperature, T_c (°C)	Electrical Efficiency, η_{pv} (%)
0	58.67	10.18
0.0005	48.27	10.74
0.00075	41.98	11.08
0.001	38.53	11.27
0.002	33.33	11.55
0.003	31.54	11.65
0.004	30.60	11.70
0.005	30.02	11.73

Table 4.15 Results of PV Temperature and PV Efficiency of Spiral Absorber under $800W/m^2$ Solar Irradiance

Mass Flow Rate, \dot{m} (kg/s)	PV Temperature, T_c ($^{\circ}C$)	Electrical Efficiency, η_{pv} (%)
0	59.13	10.16
0.0005	50.11	10.64
0.00075	43.18	11.02
0.001	39.34	11.23
0.002	33.65	11.53
0.003	31.76	11.63
0.004	30.79	11.69
0.005	30.21	11.72

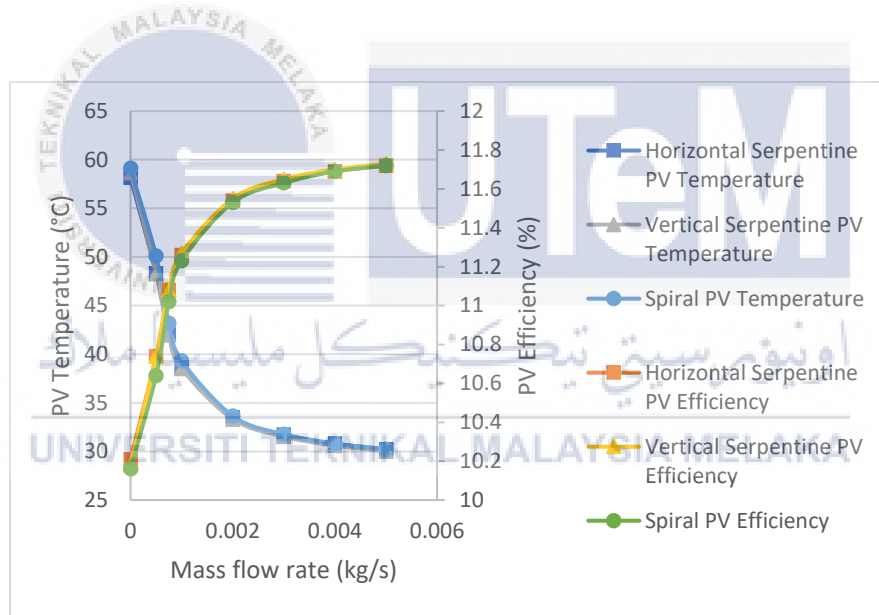


Figure 4.13 Changes in PV Temperature and PV Efficiency with Various Mass Flow Rate under $800W/m^2$ Solar Irradiance

Based on Figure 4.13, the trend of changes in PV temperature and PV efficiency under $800W/m^2$ solar irradiance is same as the graph of $1000W/m^2$ solar irradiance. The PV efficiencies under $800W/m^2$ solar irradiance were slightly higher than PV under $1000W/m^2$ solar irradiance.

Table 4.16 Results of PV Temperature and PV Efficiency of Horizontal Serpentine Absorber under 600W/m² Solar Irradiance

Mass Flow Rate, \dot{m} (kg/s)	PV Temperature, T_c (°C)	Electrical Efficiency, η_{pv} (%)
0	50.22	10.64
0.0005	42.39	11.06
0.00075	37.84	11.31
0.001	35.38	11.44
0.002	31.68	11.64
0.003	30.41	11.71
0.004	29.74	11.74
0.005	29.33	11.77

Table 4.17 Results of PV Temperature and PV Efficiency of Vertical Serpentine Absorber under 600W/m² Solar Irradiance

Mass Flow Rate, \dot{m} (kg/s)	PV Temperature, T_c (°C)	Electrical Efficiency, η_{pv} (%)
0	50.81	10.61
0.0005	42.47	11.06
0.00075	37.86	11.31
0.001	35.36	11.44
0.002	31.59	11.64
0.003	30.29	11.71
0.004	29.61	11.75
0.005	29.19	11.77

Table 4.18 Results of PV Temperature and PV Efficiency of Spiral Absorber under $600W/m^2$ Solar Irradiance

Mass Flow Rate, \dot{m} (kg/s)	PV Temperature, T_c ($^{\circ}C$)	Electrical Efficiency, η_{pv} (%)
0	51.37	10.58
0.0005	43.95	10.98
0.00075	38.82	11.25
0.001	36.02	11.40
0.002	31.86	11.63
0.003	30.47	11.70
0.004	29.77	11.74
0.005	29.34	11.77

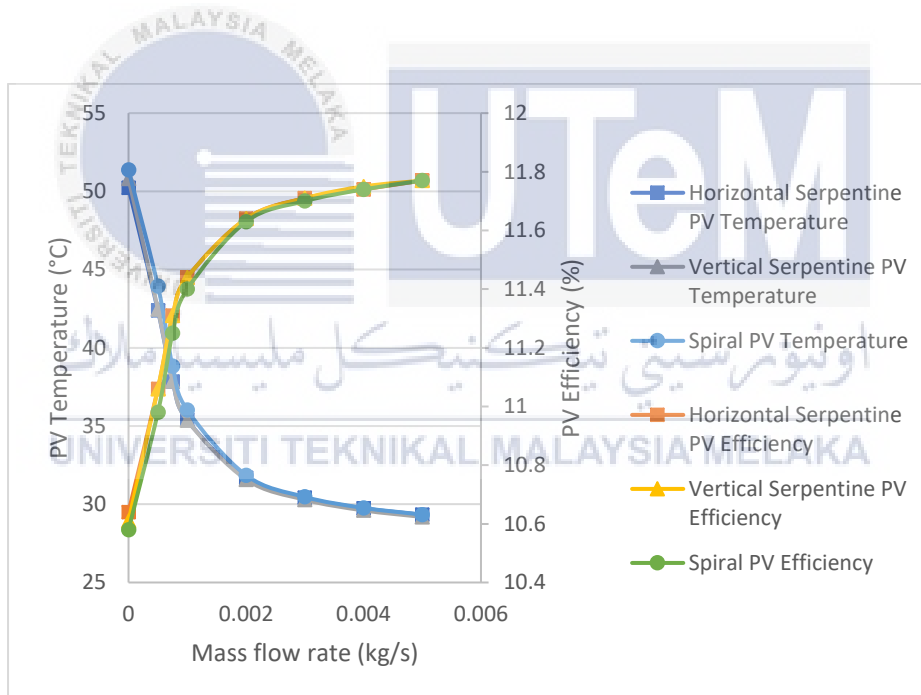


Figure 4.14 Changes in PV Temperature and PV Efficiency with Various Mass Flow Rate under $600W/m^2$ Solar Irradiance

Based on Figure 4.14, the trend of changes in PV temperature and PV efficiency under $600W/m^2$ solar irradiance is same as under $1000W/m^2$ solar irradiance. The PV efficiencies under $600W/m^2$ solar irradiance were higher than PV under $1000W/m^2$ and $800W/m^2$ solar irradiance. The increasing of mass flow rate increased the cooling effect to the PV panels, therefore as the mass flow rate increase, the PV temperature decrease.

4.3 Influence of Radiation on PVT

Figure 4.7 - 4.9 show the efficiencies of PVT with different design of absorber tube after exposure to $600W/m^2$ - $1000W/m^2$ of solar irradiance at mass flow rate of 0.005 kg/s.

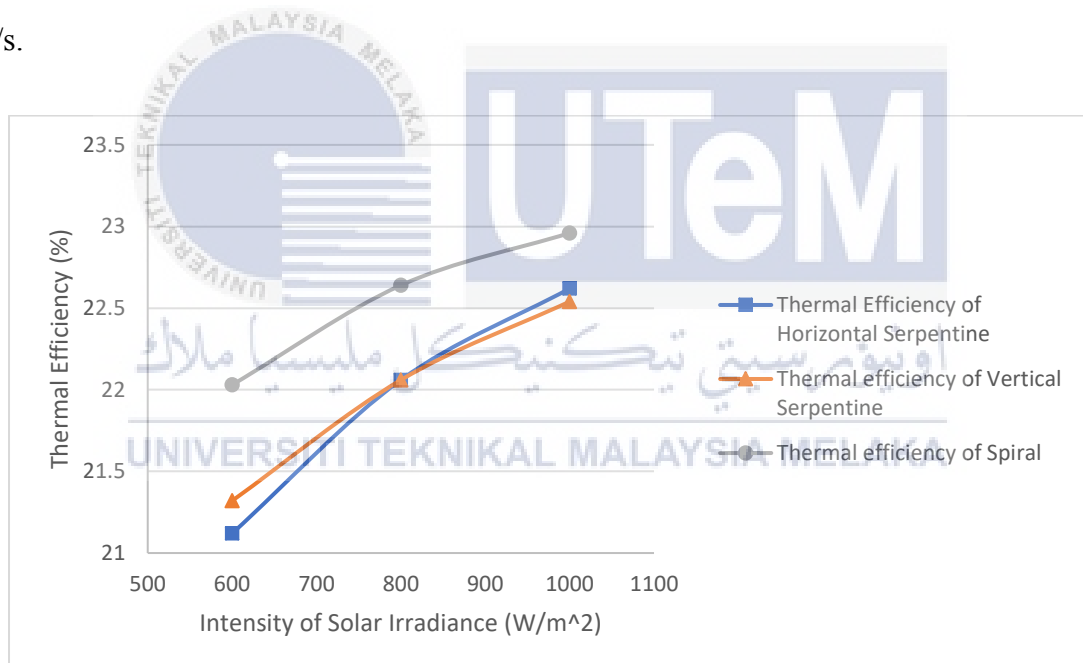


Figure 4.15 Evolution of Thermal Efficiency with Intensity of Solar Irradiance at Mass Flow Rate of 0.005 kg/s

According to Figure 4.15, thermal efficiency of spiral absorber is obviously higher than the other two designs under three different intensity of solar irradiance. At $600W/m^2$, vertical serpentine absorber had higher thermal efficiency than horizontal serpentine. When the intensity increased to $800W/m^2$, thermal efficiencies of both serpentine absorber design

were almost the same. As the intensity of solar irradiance reached $1000W/m^2$, the thermal efficiency of horizontal serpentine absorber exceeded the thermal efficiency of vertical serpentine absorber. Hence, vertical serpentine absorber design is more suitable to use at lower solar irradiance intensity, while horizontal serpentine absorber design is more suitable to use at higher solar irradiance in term of thermal efficiency.

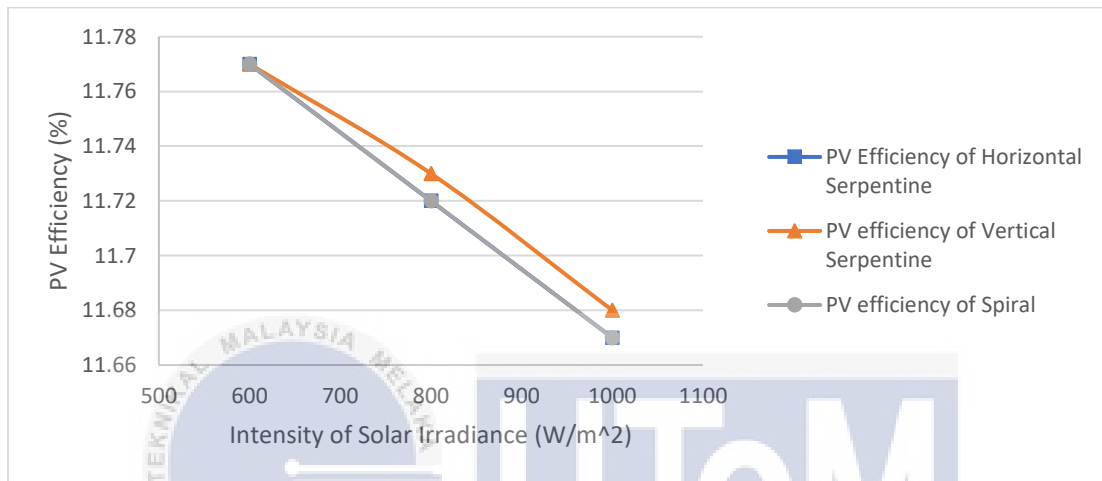


Figure 4.16 Evolution of PV Efficiency with Intensity of Solar Irradiance at Mass Flow Rate of 0.005 kg/s

In Figure 4.16, the graph only shows 2 lines because the line of spiral absorber is overlaps with the line of horizontal serpentine. At $600W/m^2$ solar irradiance, the PV efficiencies of three designs of absorber were almost the same. As the intensity of solar irradiance increased, the difference between vertical serpentine absorber and both of horizontal serpentine and spiral became more significant.

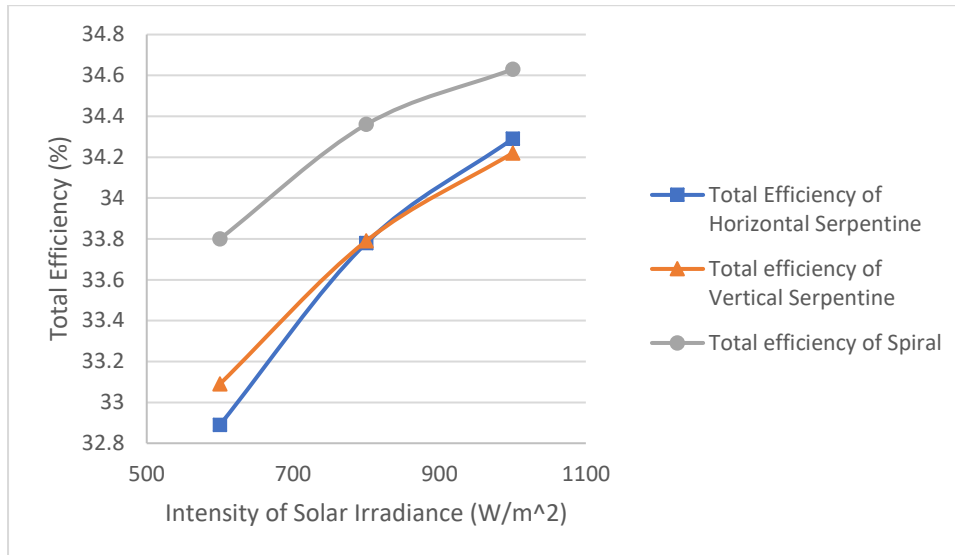


Figure 4.17 Evolution of Total Efficiency with Intensity of Solar Irradiance at Mass Flow Rate of 0.005 kg/s

The pattern of graph in Figure 4.17 is very close to Figure 4.15. This means that the thermal efficiency play an important role in total efficiency. The spiral absorber had the highest total efficiency at three different intensity of solar irradiance. At $600W/m^2$, vertical serpentine absorber had second highest total efficiency while horizontal serpentine absorber had lowest total efficiency. When the intensity of solar irradiance increased to $1000W/m^2$, the total efficiency of horizontal serpentine absorber became the second highest total efficiency and total efficiency of vertical serpentine absorber became the lowest total efficiency.

4.4 Performance of PVT

The total efficiency of PVT represents the performance of PVT. Total efficiency is the sum of the thermal efficiency and PV efficiency. Figure 4.18, 4.19 and 4.20 shows the total efficiency of three different design under three different solar irradiance intensities.

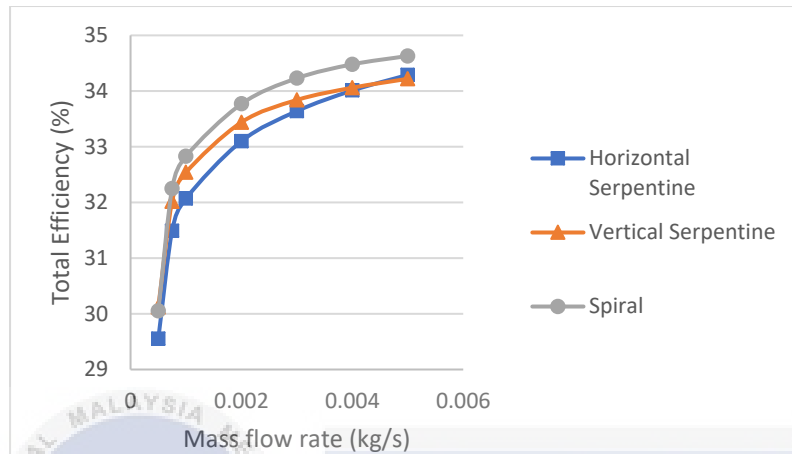


Figure 4.18 Evolution of Total Efficiency under $1000W/m^2$ Solar Irradiance Intensity

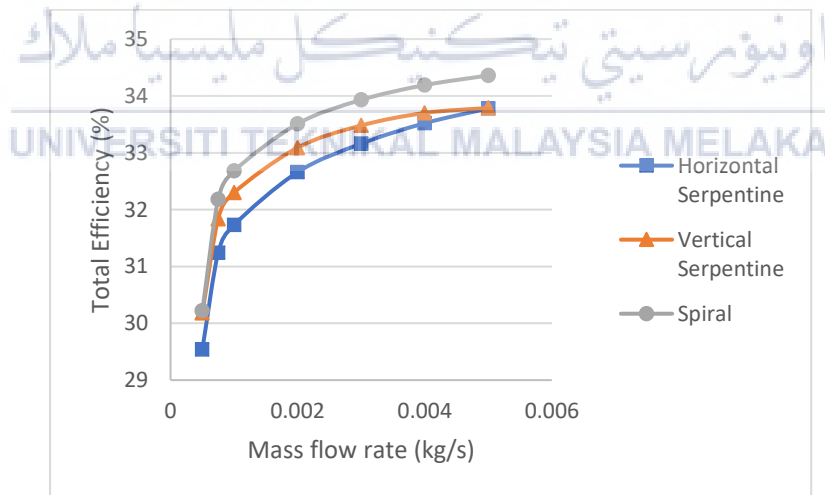


Figure 4.19 Evolution of Total Efficiency under $800W/m^2$ Solar Irradiance Intensity

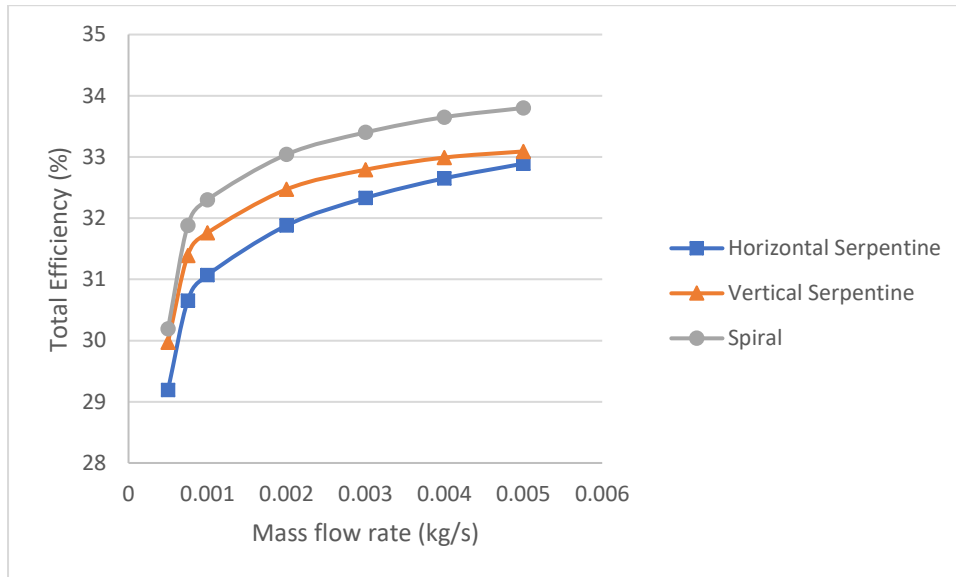


Figure 4.20 Evolution of Total Efficiency under $600W/m^2$ Solar Irradiance Intensity

The spiral absorber PVT had the highest total efficiency among the three different design of absorber, from 30.05% to 34.63%. It followed by vertical serpentine absorber PVT, from 30.12% to 34.22%. The PVT which has lowest total efficiency is PVT with horizontal serpentine design of absorber, from 29.55% to 34.29. At 0.005 kg/s, total efficiency of horizontal serpentine started to exceed total efficiency of vertical serpentine, became the second highest total efficiency.

CHAPTER 5

CONCLUSION AND RECOMMENDATIONS

5.1 Conclusion

This study focuses on investigating and comparing the thermal efficiency, electrical efficiency and total efficiency of PVTs with different design of absorber. The results obtained from simulation under steady state condition.

From the comparison of thermal efficiency, the effect of mass flow rate is greater than effect of temperature difference between inlet and outlet on thermal efficiency. The increase rate of thermal efficiency with increasing mass flow rate is lower at higher mass flow rate. Hence, there is not necessary to increase mass flow rate to improve the thermal efficiency when the thermal efficiency was approached to a constant. For the PV efficiency, it showed the same trend as thermal efficiency, the increase rate of PV efficiency was become lower at higher mass flow rate. The simulation of PVT exposed to different intensity of solar irradiance showed that the higher the solar irradiance, the higher thermal efficiency and lower PV efficiency.

The comparison of performance of PVT with different design of absorber tube exhibited that the spiral absorber had the highest of total efficiency at most of the mass flow rate. Horizontal serpentine absorber had the second highest total efficiency and followed by vertical serpentine.

5.2 Recommendations

Due to the limitation of time and performance of simulation device, only PVT with partial length of absorber tube were simulated since this study is to prove which design of absorber tube is better. Further research can be done to obtain the results of the PVT with full length of absorber and same design of absorber as in this study. Thus, the performance of the designed PVT can be compare with the other existing PVT.

Moreover, further research can be done to obtain the results on wider range of variables. This study only done simulation from 0.0005kg/s to 0.005kg/s mass flow rate. For example, Figure 4.18 showed that total efficiency of serpentine horizontal absorber started to exceed total efficiency of vertical serpentine at 0.005kg/s. Hence, at further mass flow rate may have useful finding on performance of PVT.

Apart from that, an experiment with the setup which same as the simulation setup in current research is recommended to carry out to validate the simulation results. This could strengthen the reliability of the simulation results in current research.

REFERENCES

- Allan, J., Dehouche, Z., Stankovic, S., & Mauricette, L. (2015). Performance testing of thermal and photovoltaic thermal solar collectors. *Energy Science & Engineering*, 3(4), 310–326. <https://doi.org/10.1002/ese3.75>
- Chow, T. T. (2010). A review on photovoltaic/thermal hybrid solar technology. *Applied Energy*, 87(2), 365–379. <https://doi.org/10.1016/j.apenergy.2009.06.037>
- Corbin, C. D., & Zhai, Z. J. (2010). Experimental and numerical investigation on thermal and electrical performance of a building integrated photovoltaic-thermal collector system. *Energy and Buildings*, 42(1), 76–82. <https://doi.org/10.1016/j.enbuild.2009.07.013>
- Daghigh, R., Ibrahim, A., Jin, G. L., Ruslan, M. H., & Sopian, K. (2011). Predicting the performance of amorphous and crystalline silicon based photovoltaic solar thermal collectors. *Energy Conversion and Management*, 52(3), 1741–1747. <https://doi.org/10.1016/j.enconman.2010.10.039>
- Huang, B. J., Lin, T. H., Hung, W. C., & Sun, F. S. (2001). Performance evaluation of solar photovoltaic/thermal systems. *Solar Energy*, 70(5), 443–448. [https://doi.org/10.1016/S0038-092X\(00\)00153-5](https://doi.org/10.1016/S0038-092X(00)00153-5)
- Ibrahim, A., Fudholi, A., Sopian, K., Othman, M. Y., & Ruslan, M. H. (2014). Efficiencies and improvement potential of building integrated photovoltaic thermal (BIPVT) system. *Energy Conversion and Management*, 77, 527–534. <https://doi.org/10.1016/j.enconman.2013.10.033>
- Ibrahim, A., Othman, M. Y., Ruslan, M. H., Alghoul, M. A., Yahya, M., Zaharim, A., & Sopian, K. (2009). Performance of photovoltaic thermal collector (PVT) with different absorbers design. *WSEAS Transactions on Environment and Development*, 5(3), 321–330.
- Ji, J., Lu, J. P., Chow, T. T., He, W., & Pei, G. (2007). A sensitivity study of a hybrid photovoltaic/thermal water-heating system with natural circulation. *Applied Energy*, 84(2), 222–237. <https://doi.org/10.1016/j.apenergy.2006.04.009>

- Khan, F., Singh, S. N., & Husain, M. (2010). Effect of illumination intensity on cell parameters of a silicon solar cell. *Solar Energy Materials and Solar Cells*, 94(9), 1473–1476. <https://doi.org/10.1016/j.solmat.2010.03.018>
- Khelifa, A., Touafek, K., Ben Moussa, H., & Tabet, I. (2016). Modeling and detailed study of hybrid photovoltaic thermal (PV/T) solar collector. *Solar Energy*, 135, 169–176. <https://doi.org/10.1016/j.solener.2016.05.048>
- Kim, J. H., & Kim, J. T. (2012). Comparison of electrical and thermal performances of glazed and unglazed PVT collectors. *International Journal of Photoenergy*, 2012. <https://doi.org/10.1155/2012/957847>
- Nahar, A., Hasanuzzaman, M., & Rahim, N. A. (2017). A Three-Dimensional Comprehensive Numerical Investigation of Different Operating Parameters on the Performance of a Photovoltaic Thermal System With Pancake Collector. *Journal of Solar Energy Engineering*, 139(3), 31009. <https://doi.org/10.1115/1.4035818>
- Senthil Kumar, R., Puja Priyadharshini, N., & Natarajan, E. (2015). Experimental and Computational Fluid Dynamics (CFD) Study of Glazed Three Dimensional PV/T Solar Panel with Air Cooling. *Applied Mechanics and Materials*, 787, 102–106. <https://doi.org/10.4028/www.scientific.net/AMM.787.102>
- Skoplaki, E., & Palyvos, J. A. (2009). On the temperature dependence of photovoltaic module electrical performance: A review of efficiency/power correlations. *Solar Energy*, 83(5), 614–624. <https://doi.org/10.1016/j.solener.2008.10.008>
- Struckmann, F. (2008). Analysis of a Flat-Plate Solar Collector. *Mokslas - Lietuvos Ateitis*, 3, 39–43. <https://doi.org/10.3846/mla.2011.108>
- Stylianou, S. (2016). Thermal Simulation of Low Concentration PV/Thermal System using a Computational Fluid Dynamics Software. *Repository.Tudelft.Nl*. Retrieved from <http://repository.tudelft.nl/islandora/object/uuid:0da53df4-df77-4afd-9bc0-89ccca593719/datastream/OBJ/download>

Tripanagnostopoulos, Y. (2007). Aspects and improvements of hybrid photovoltaic/thermal solar energy systems. *Solar Energy*, 81(9), 1117–1131. <https://doi.org/10.1016/j.solener.2007.04.002>





Appendix A

PSM I Gantt Chart

No.	Topic	Weeks													
		1	2	3	4	5	6	7	8	9	10	11	12	13	14
1.	Journal Reading	█	█	█	█	█	█	█	█	█	█	█	█	█	█
2.	Identify Suitable Topic for PSM	█	█	█	█	█	█	█	█	█	█	█	█	█	█
3.	Learn Basic of ANSYS	█	█	█	█	█	█	█	█	█	█	█	█	█	█
4.	Geometry Drawing	█	█	█	█	█	█	█	█	█	█	█	█	█	█
5.	Meshing Geometry	█	█	█	█	█	█	█	█	█	█	█	█	█	█
6.	Setup of Simulation FLUENT	█	█	█	█	█	█	█	█	█	█	█	█	█	█
7.	Run Simulation FLUENT	█	█	█	█	█	█	█	█	█	█	█	█	█	█
8.	Preparation of Methodology	█	█	█	█	█	█	█	█	█	█	█	█	█	█
9.	Report Writing	█	█	█	█	█	█	█	█	█	█	█	█	█	█
10.	Submission of PSM I Report	█	█	█	█	█	█	█	█	█	█	█	█	█	█

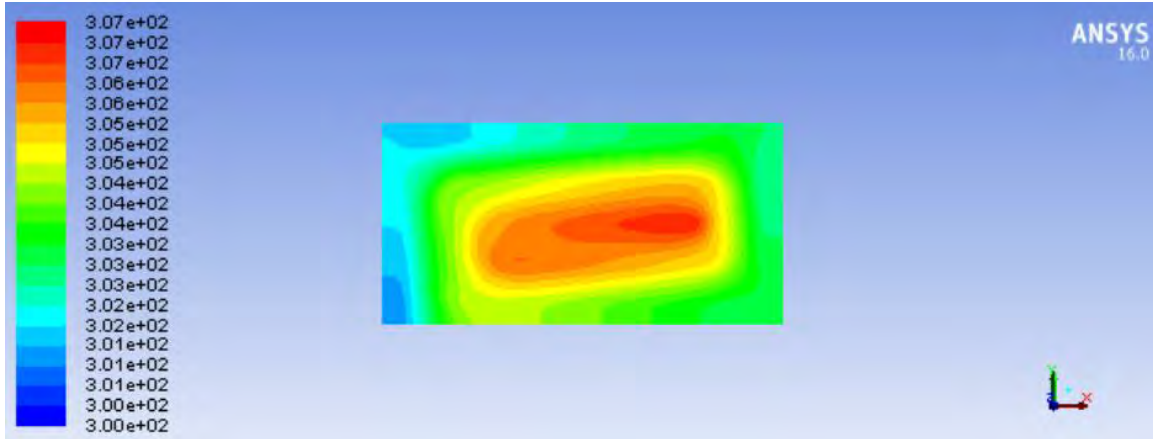
Appendix B

PSM II Gantt Chart

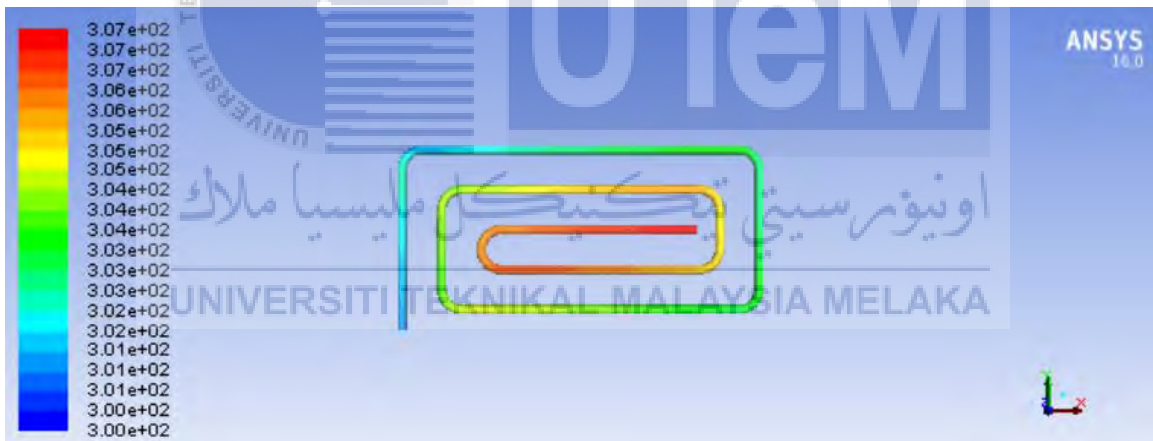
No.	Topic	Weeks													
		1	2	3	4	5	6	7	8	9	10	11	12	13	14
1.	Design Absorber Tube of PVT	■													
2.	Geometry Drawing							■							
3.	Run Simulation of Horizontal Serpentine Absorber PVT														
4.	Run Simulation of Vertical Serpentine Absorber PVT														
5.	Run Simulation of Spiral Absorber PVT														
6.	Tabulation of Results														
7.	Graph Plotting														
8.	Report Writing														
9.	Submission of PSM II Draft Report														

Appendix C

Contour Diagram of PV of spiral absorber PVT at 0.005 kg/s under $1000W/m^2$ solar irradiance

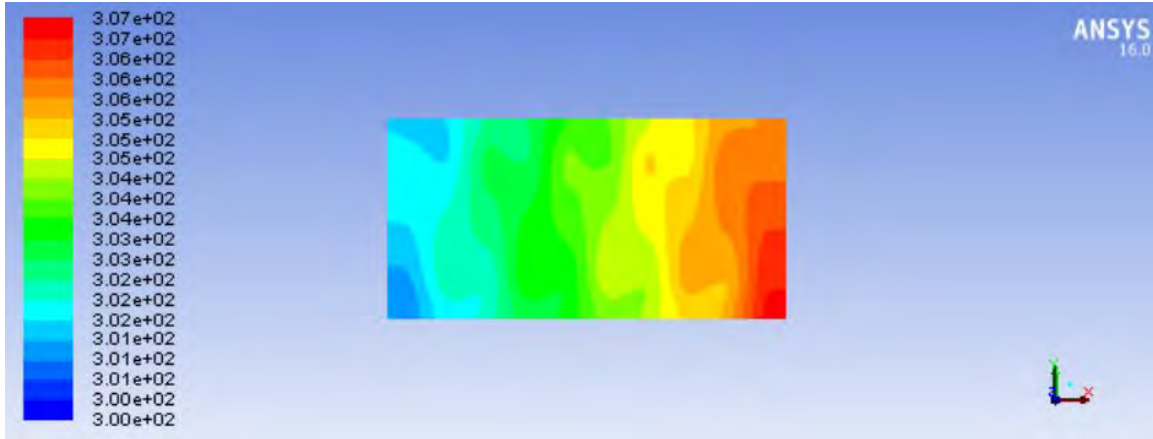


Contour Diagram of water surface of spiral absorber PVT at 0.005 kg/s under $1000W/m^2$ solar irradiance

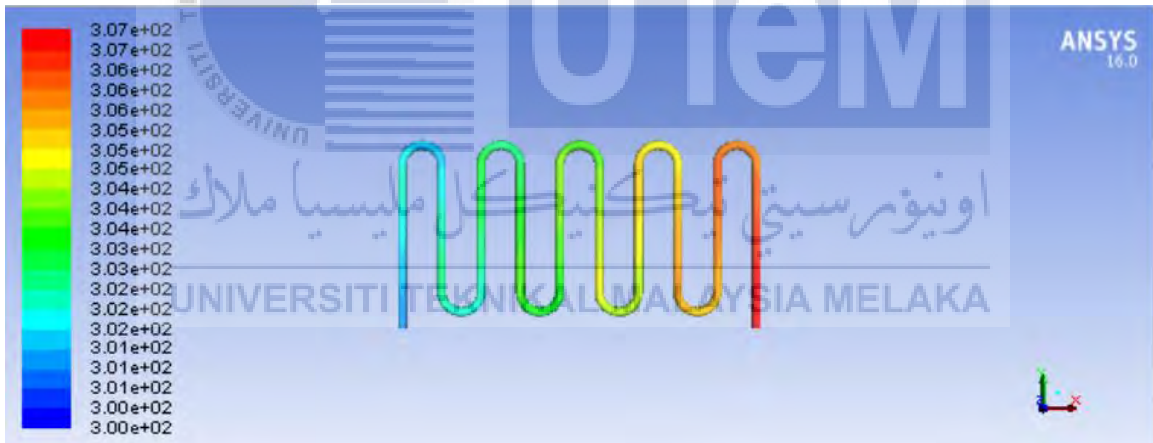


Appendix D

Contour Diagram of PV of vertical serpentine absorber PVT at 0.005 kg/s under $1000W/m^2$ solar irradiance

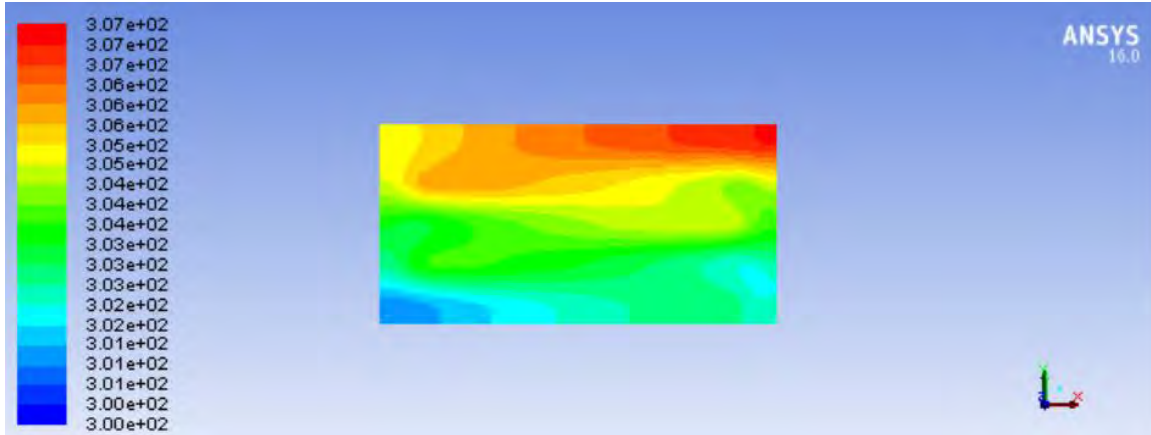


Contour Diagram of water surface of vertical serpentine absorber PVT at 0.005 kg/s under $1000W/m^2$ solar irradiance



Appendix E

Contour Diagram of PV of horizontal serpentine absorber PVT at 0.005 kg/s under $1000W/m^2$ solar irradiance

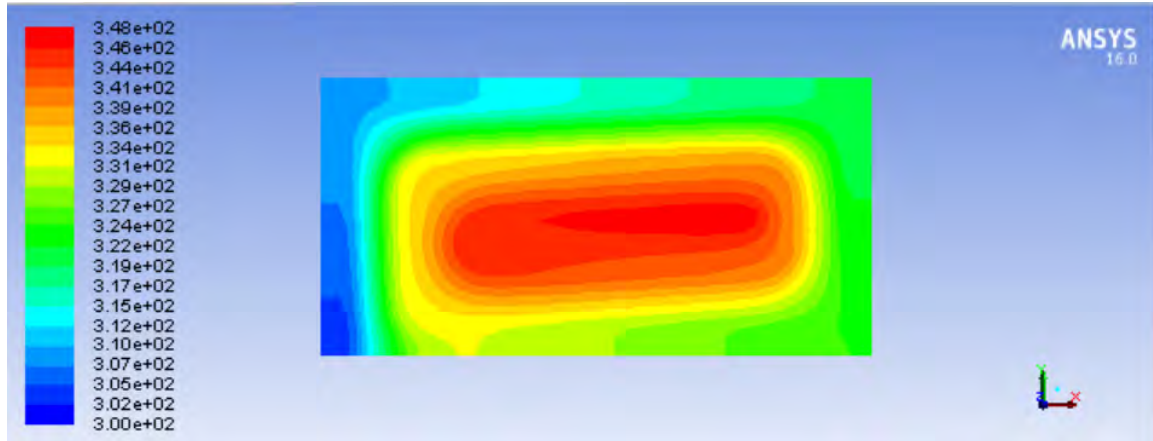


Contour Diagram of water surface of horizontal serpentine absorber PVT at 0.005 kg/s under $1000W/m^2$ solar irradiance



Appendix F

Contour Diagram of PV of spiral absorber PVT at 0.0005 kg/s under $1000W/m^2$ solar irradiance

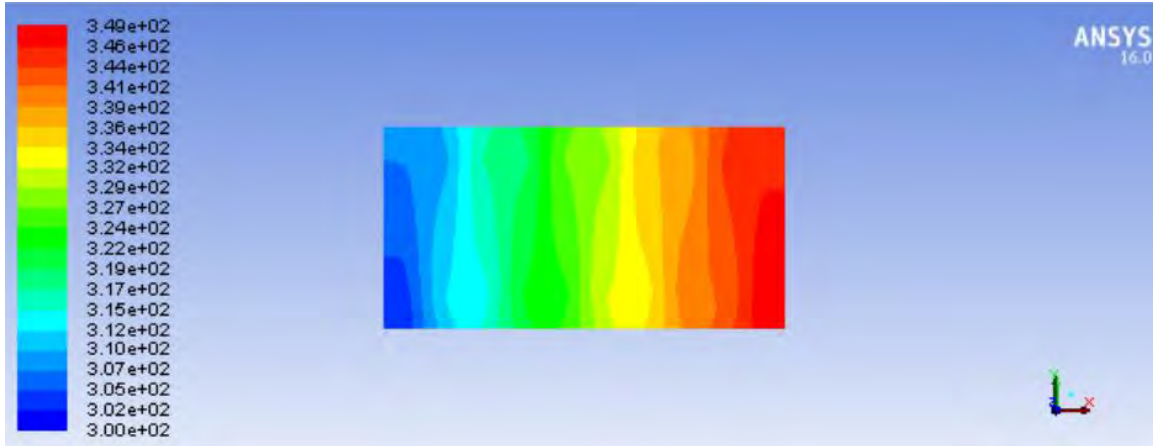


Contour Diagram of water surface of spiral absorber PVT at 0.0005 kg/s under $1000W/m^2$ solar irradiance

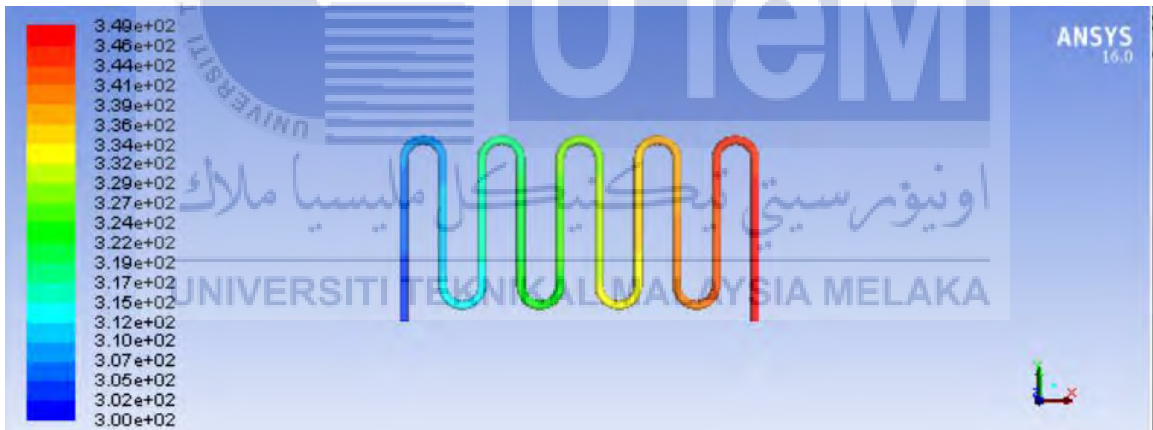


Appendix G

Contour Diagram of PV of vertical serpentine absorber PVT at 0.0005 kg/s under $1000W/m^2$ solar irradiance

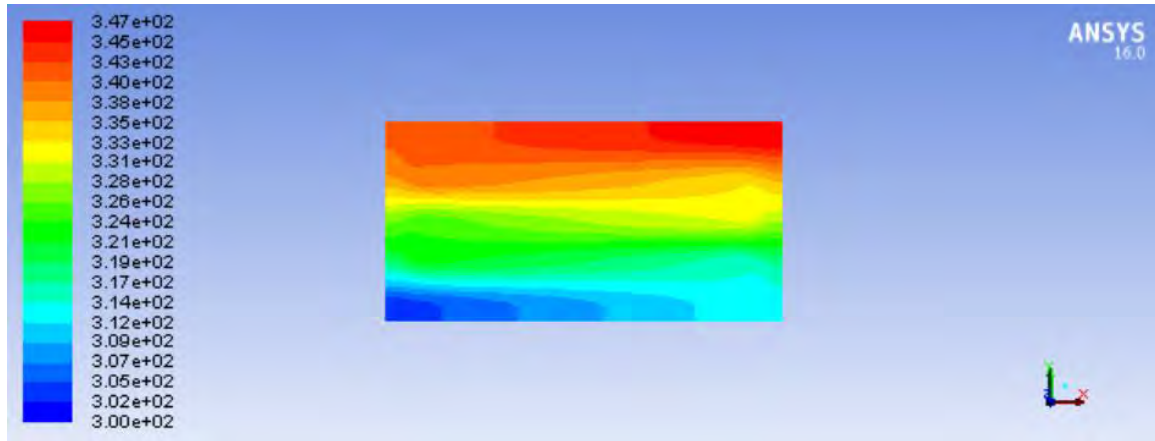


Contour Diagram of water surface of vertical serpentine absorber PVT at 0.0005 kg/s under $1000W/m^2$ solar irradiance



Appendix H

Contour Diagram of PV of horizontal serpentine absorber PVT at 0.0005 kg/s under $1000W/m^2$ solar irradiance



Contour Diagram of water surface of horizontal serpentine absorber PVT at 0.0005 kg/s under $1000W/m^2$ solar irradiance

